APPLICATION OF A NEW TECHNIQUE FOR RADIO WAVE PROPAGATION STUDY TO EXPERIMENTAL CONFIRMATION OF THE PHASE CHARACTERISTIC OF NORTON'S GROUND WAVE PROPAGATION THEORY

Thesis by

Eberhardt Rechtin

In Partial Fulfillment of the Requirements

For the Degree of

Doctor of Philosophy

California Institute of Technology

Pasadena, California

1950

ABSTRACT

The basic purpose of this work is to investigate experimentally the phase characteristics of radio waves propagated along the surface of the earth as proposed by K.A. Norton (reference 1). Norton's theory indicates that the ground wave phase at distances of the order of tens of miles is greater than the corresponding space wave phase by not more than 180 degrees. From a radio surveying point of view, range errors of tens of feet may result. To avoid difficulties inherent in the direct and absolute approach, that of comparison of optical surveying with radio surveying over actual terrain at normally used frequencies (200 kilocycles per second to 15 megacycles per second), a new technique is developed.

It is proposed that the propagation of radio waves may be studied by use of appropriate scale models, permitting experiments otherwise impossible because of the gigantic size of the equivalent true scale systems. Further, relative measurements may be obtained directly in a model system by proper choice of paths as contrasted with the absolute measurements usually made in a full-scale system.

The technique is demonstrated by a preliminary experimental confirmation of Norton's theory. Suggestions for technique improvement and for further investigation possibilities are given.

ACKNOWLEDGEMENTS

The fact that this work was accomplished at all is due to the inspiring cooperation of many people. My highest gratitude is due to Doctor W.H. Pickering, Professor of Electrical Engineering at CalTech, for his continuous interest and encouragement. It was my pleasure and good fortune to have the assistance of Lt. Col. Robert W. Paulson USAF and Capt. James H. Watkins USAF of the graduate school. Their good humor and engineering judgment solved many a problem.

The blank-check assistance of the range instrumentation section under Mr. Fred Arndt at NAMTC, Pt. Mugu, enabled us to do our work in the minimum time with the fewest obstacles. Messrs. Newell and Knott of this section furnished everything requested from rowboat oars to BOQ accomodations.

The immediate approval for use of the facilities of the Pasadena City College Technology Department under Mr. Moses made the completion of this research possible. The somewhat unusual request to permit dissolving a half ton of salt in their mirror pond was not questioned.

My special thanks are due to Dr. W.R. Smythe, Professor of Physics at CalTech, Mr. Paul Reedy and Mr. Robert Benton of the Jet Propulsion Laboratories, and Miss Deedee Denebrink of Scripps College for invaluable discussions and suggestions. It is the help of such people that makes research profitable, interesting, and enjoyable.

LIST OF SYMBOLS USED IN TEXT

b, b', b''	Angle parameters in Norton's theory depending primarily upon ground constants
B	b modified by the reflection coefficient, R.
E, E_o	Field strength
f_{mc}	Frequency in megacycles/sec.
h_A	Height of horn A, etc., measured from grount to center of horn
i	$\sqrt{-1}$
k_{AB}	Amplitude of received signal from horn at horn B mouth
k_B	Attenuator action of horn and coaxial system B
p	Norton's (and Sommerfeld's) "numerical distance"
P	p modified by the reflection coefficient, R.
q_1	numerical antenna 1
r_1	Norton's symbol for slant range from transmitter antenna to receiver antenna
r_2	Norton's symbol for slant range from transmitter image antenna to receiver antenna
r_{AB}	Slant range from horn A to horn B
r'_{AB}	Slant range from image horn A to horn B
R	Plane wave reflection coefficient
t	time
x, χ	Horizontal range between transmitting and receiving horns
X, $\mathfrak{X}$	Ground constant parameter
y	Vertical height variable used in water depth problem
y_o	Water depth

LIST OF SYMBOLS, CONTINUED

α	Propagation attenuation constant of conducting medium
β	Propagation phase constant of dielectric
γ_B	Phase angle of line B to receiver, horn D connected
γ_D	Phase angle of line D to receiver, B connected
ε	Dielectric constant
θ_{AB}	Total propagation phase angle between horn mouth A and horn mouth B
θ_A	Variable phase angle at receiver used to compare phases of horns B and D when transmitting from horn A
θ_C	Variable phase angle at receiver used to compare phases of horns B and D when transmitting from horn C
λ	Wave length
σ_{emu}	Conductivity in electromagnetic units
σ	Conductivity in mhos per meter
ϕ	"Norton phase shift", a function of P and B, and the subject of this thesis
ω	$2\pi f_{mc}$

LIST OF FIGURES

TABLE OF CONTENTS

TABLE OF CONTENTS (CONT.)

I. PROPAGATION THEORY UNDER INVESTIGATION

With the advent of radio wave broadcasting much theory was presented concerning the calculation of ground-wave field intensities. The theory was well summarized by K.A. Norton in 1941 (ref. 1). Very recently the theory has become of greater interest in the fields of radio wave surveying (Doppler radar, Shoran, etc.) and of radio wave propagation velocity measurement. Norton's work, in particular, proposed the following solution to the propagation equation:

$$1)\quad E = \frac{E_0}{x}\Big[\cos^3\psi_1\, e^{i\frac{2\pi r_1}{\lambda}} + R\cos^3\psi_2\, e^{i\frac{2\pi r_2}{\lambda}} + (1-R)f(P,B)\cos^2\psi_2\, e^{i\left(\frac{2\pi r_2}{\lambda}+\phi\right)}\Big]$$

The quantities x, r_1, r_2, h_1, h_2, ψ_1, and ψ_2 are defined in figure 1. E and E_0/x are to be expressed in the same units, $i = \sqrt{-1}$, and all lengths are to be expressed in centimeters. R is the plane wave reflection coefficient of the ground, given by:

$$2)\quad R = |R|e^{i\phi_R} = \frac{\frac{g_1+g_2}{2p}\, e^{i\left(\frac{\pi}{4}-\frac{b}{2}\right)} - 1}{\frac{g_1+g_2}{2p}\, e^{i\left(\frac{\pi}{4}-\frac{b}{2}\right)} + 1}$$

where

$$3)\quad p = \frac{\pi r_2}{\lambda}\;\frac{\cos^2 b''}{X\cos b'}$$

4a) $b' = \tan^{-1}\left[(\varepsilon/X) - \frac{\cos^2\psi_2}{X}\right]$

4b) $b'' = \tan^{-1}(\varepsilon/X)$

4c) $b = 2b'' - b$

5) $q_{1,2} = \frac{2\pi h_{1,2}}{\lambda}\left[\frac{\cos^2 b''}{X \cos b'}\right]^{\frac{1}{2}}$

6) $X = \frac{1.79731 \times 10^{15} \sigma_{e.m.u.}}{f_{m.c.}}$

$\sigma_{e.m.u.}$ = ground conductivity in electromagnetic units

$f_{m.c.}$ = frequency in megacycles per second

7) $P = \frac{4p}{(1 - R)^2}$

8) $B = b - 2\phi_{1-R}$

f(P,B) is given by Norton graphically on page 624 (ref. 1) and is repeated here for convenience in figure 2a.

ϕ is the associated phase shift, repeated here in figure 2b.

R is given in figure 2c for sea water at 3000 mc. (ref. 2).

For very low antenna heights (vertical polarization assumed throughout) $R \to -1$, $\cos^3\psi_2 \to 1$, $r_2 \to r_1 \to x$, $f(P,B) \to f(p,b)$ and

9) $E \to \frac{E_0}{x} f(p,b) e^{i\left(\frac{2\pi x}{\lambda} + \phi\right)}$ (surface wave equation)

Equation 9) is extensively used in radio surveying. By measuring the phase between transmitter and receiver it is possible to find the distance x to very high orders of accuracy-- far higher than a first-order optical survey. Range errors may be reduced by a knowledge of the function ϕ. Lacking a knowledge of both absolute phase and of precise distance, however, an experimental check has been difficult. Surveying operating frequencies are of the order of five to twenty megacycles per second. Confirmation of Norton's predicted ϕ would require a one hundred mile range over sea water or a four mile range over land. In the first case, transit surveying to within a desired five foot tolerance is impossible; in the second case, a reflection-free area with uniform ground conditions over the propagation path is rare.

II. THEORETICAL INVESTIGATION OF EXPERIMENTAL TECHNIQUES

A. Two possible approaches

1. Method 1 (absolute phase measurement). There are many systems which might be suggested; basically all are variations of the system shown in figure 3. The coaxial line and associated equipment must have a VSWR (voltage standing wave ratio) of very nearly unity; the frequency of the source must be constant to 1:100,000; distances must be measured to 1:100,000; and all constant phases introduced by the equipment must be accurately known. There is little advantage in attempting to use an as-yet-undeveloped, frequency stable, coherent local oscillator to replace the coaxial line. There is no point in using modeling techniques-- accuracies required are still 1:100,000 and are just as difficult to achieve.

2. Method 2 (relative phase measurement). Most propagation problems are interested in the behavior of radio waves as compared with the free space behavior. The deviations from such free space behavior are small but quite important. It is therefore logical to attempt to measure the deviations directly by setting up two paths of very nearly equal distance, one of which closely approximates free space conditions, the other of which incorporates the features of interest-- reflecting objects, diffracting ridges, or, in this case, conducting surfaces parallel to the direction of travel.

Preliminary investigations of the characteristics of the surface wave show that its field strength decreases very rapidly with height above the surface. Thus one path close to the surface and one high above it are indicated. The method shown in figure 4 is best visualized as comparing the phase between horns A and B with that between C and D. Heights h_C and h_D should be at least ten wavelengths; heights h_A and h_B should be one-half wavelength or less.

Propagation from horn C to horn D may take two paths, a direct one and one reflecting from the surface. The free space criterion may be achieved and the percentage of surface wave associated with path CD reduced by proper selection of distances CD. Readings are taken only at points of maximum signal E_{CD}. It is apparent that the maximum signal occurs only when the reflected ray is in phase with the direct ray (and when the phase is that of free space). The associated surface wave at such maximum signal points is at least 25 decibels down.

Norton's work indicates that the amplitude and phase characteristics of the surface wave are functions of r/λ and of σ. The difficulties associated with construction of movable, vertically true, mounting towers ten wavelengths high are eliminated by model techniques. Instead of the normally used 10 megacycles/sec., a frequency of 3000 megacycles/sec. was chosen. Propagation over water was found to result in convenient distance limits. Ice, for example, considerably shortened the range (p = 100 at about 10 feet); metal lengthened it to impractical distances. A frequency of 10,000 megacycles/sec. was discarded because the range was shortened by two-thirds and all construction accuracies were correspondingly increased. At 3000 megacycles per second, accuracy to within a millimeter is sufficient, but at 10,000 megacycles/sec., one third of a millimeter accuracy is required to achieve the same result.

It is interesting to note that wholly from geometrical considerations the distance "points" of maximum E_{CD} are quite broad. Measurement of the location of the maxima to one centimeter results in phase errors of less than one degree. In the absolute system (method 1) a distance error of one centimeter would mean a 36 degree phase error. Tolerances will be discussed later in more detail.

B. Investigation of the relative phase technique

1. Detailed description. Because of a complex interrelationship between signal strengths E_{AB}, E_{AD}, E_{CB}, and E_{CD} and their associated phase angles, it is not readily possible to subtract θ_{CD} from θ_{AB} directly (see previous section) by transmitting through horns A and B and receiving at horns C and D simultaneously. Lacking 0.2° beam width horns, it is doubtful if a direct measurement of ϕ is possible. It is questionable, even so, if an attempt to do so is advisable. The system would have to have a VSWR of unity throughout, would of necessity be complex, and would require constant checks on its operating performance.

The solution, fortunately, is both simple and advantageous. First, transmit with horn A and compare phases θ_{AB} and θ_{AD}.

This is accomplished by mixing the nearly-equal signals from horns B and D at a crystal. A variable phase angle, θ_A, is so adjusted that a minimum resultant signal is detected. This minimum will occur at points of phase opposition of signals E_{AB} and E_{AD}. Second, transmit with horn C and compare phases θ_{CB} and θ_{CD}, resulting in θ_C. Maintenance of geometrical symmetry insures $\theta_{AD} = \theta_{CB}$. Then, subtract θ_c from θ_A to obtain

$$10)\quad \theta_A - \theta_c = (\theta_{AB} - \theta_{AD}) - (\theta_{CD} - \theta_{CB})$$
$$= \theta_{AB} - \theta_{CD} = \phi$$

In greater detail:

<u>With the transmitter at position A</u> the signal at the receiver through horn B is

$$E_{AB} = k_{AB}k_B \sin\left[\omega t + \theta_{AB} - \theta_A + \gamma_B\right]$$

where

k_{AB} gives the amplitude at horn B input due to wave from A to B

k_B is an attenuation action in branch B

θ_{AB} is the total space phase shift

θ_A is a measurement phase shift subtracted by some phase shifting mechanism

γ_B is the phase shift in line B to the receiver, excluding θ_A, and measured with D connected

Similarly, the signal at the receiver through D from A is

$$E_{AD} = k_{AD}k_D \sin\left[\omega t + \theta_{AD} + \gamma_D\right]$$

The phase shifter, θ_A, has been assumed to be located in branch B.

The attenuators are so set that

$$k_{AB}k_B \cong k_{AD}k_D$$

Phase shift θ_A is then so adjusted that when the two signals, E_{AB} and E_{AD}, are mixed at the crystal a minimum amplitude reading occurs. At this phase shifter setting, therefore,

$$\omega t + \theta_{AB} - \theta_A + \gamma_B = \omega t + \theta_{AD} + \gamma_D + \pi$$

or

11) $$-\theta_A = \theta_{AD} - \theta_{AB} + \gamma_D - \gamma_B + \pi$$

<u>With the transmitter at position C</u>, a proper change of subscripts yields

12) $$-\theta_c = \theta_{CB} - \theta_{CD} + \gamma_D - \gamma_B + \pi$$

<u>Therefore</u>, if $r_{AD} = r_{CB}$, $\theta_{AD} = \theta_{CB}$, and

$$\theta_A - \theta_C = \theta_{AB} - \theta_{CD} = \phi\,(P,B)$$

which is the same as equation 10).

Because of the comparison method used, the phase characteristics of the transmitter coaxial lines, junctions, etc. are not important. The transmitter VSWR need not be unity other than for reasons of greater power output. Precision transmitting equipment is not necessary.

It is also advantageous to eliminate the receiver coax system phase characteristics. A phase shifting mechanism in either lines B or D will have no meaning unless the VSWR is unity. In addition, changing the amount of attenuation during a set of readings will undoubtedly add phase error to the system in an unknown manner. In other words, in terms of equations 11) and 12), the angles γ_D and γ_B must not change either during changes in θ_A and θ_C or during adjustments of attenuation.

A neat solution to the phase shifter difficulty is accomplished by moving the horns back and forth on calibrated screws. To maintain symmetry of the cross path phase angles, horn B is moved when transmitting from A and horn D is moved when transmitting from C. The distance AD is constant during the first measurement and is equal to the distance CB held constant in the second measurement. From figure 5 it is apparent that a 10 centimeter motion of the bottom horn will negligibly affect the relative phase of the surface wave with respect to the "cross-path" phase θ_{AD}. As has been mentioned previously, motion of the top horn at a broad maximum signal location will probably introduce less error than a phase shifter in a line of VSWR not equal to unity. Permissible motions are discussed later under section II B 2 b. The second difficulty, that of the attenuators adding phase error, is fortunately not too difficult of solution. Calculations of appendix A show that the amplitude of E_{AB} is to E_{AD} as the amplitude of E_{CB} is to that of E_{CD}, i.e., the amplitude of the cross path wave is approximately equal to the geometric mean ($E_{g.m.}$) of the top and bottom wave amplitudes. Thus one attenuator on horn D will suffice for any one set of measurements. If this adjustment is not changed during a set, any phase characteristics the attenuator may have will cancel out (as part of γ_D).

The foregoing discussion is illustrated in figures 5 through 8. Predicted results are shown in figure 5 for sea water ($\sigma = 5$) and for fresh water ($\sigma = 10^{-3}$). Experimentally, only distances corresponding to points of maximum E_{CD} may be used to obtain data. The distances will be different in the two cases, salt and fresh water. Figure 6 shows the relative amplitudes of E_{AB}, E_{AD}, E_{CB} (equal to E_{AD}) and E_{CD}. $E_{g,m.}$ is plotted for comparison with E_{AD}. $E_{g.m.}$ is realized physically by action of an attenuator in branch D. With the transmitter at position A an attenuator in branch D will attenuate E_{AD} with respect to E_{AB}; with the transmitter at position C an attenuator in branch D will attenuate E_{CD} with respect to E_{CB}. On a purely relative basis, E_{AB} is amplified by the same amount that E_{CD} is attenuated (see figure 6). The optimum solution (on this relative basis) occurs when $E_{AB} = E_{CD} = E_{g.m.} \cong E_{AD}$. Figure 7 shows the effect of mixing two signals of differing amplitude and phase. In all cases, of course, the minimum point occurs when the signals are in phase opposition. However, one may say that unless the two received amplitudes are equal within a factor of two, an accurate minimum resultant signal point will be difficult to observe. (In practice, the crystal detector tends to sharpen the null points.) With this in mind, one now compares E_{AD} and $E_{g.m.}$; their ratio (or inverse) is plotted in figure 8. From this figure it may be seen that the distance range of interest is useable. In actual operation a tuning stub on horn D was adjusted at each range point so that with transmission from C equal signal was received from B and D. The stub position was not changed during the rest of the measurements at that point. The ratio of signal strengths received from B and D with transmission from A resulted in satisfactory minima.

2. Physical tolerances

a. Distance: Norton's work measures all distances from antennas which are essentially point sources in size compared to the distances involved. However, in order to reduce side reflections and in order to decrease the required transmitter power in this trial system, microwave horns of reasonable size are required. The radio wave emerging from the mouth of the horn will not have a spherical wave front. For this reason the equivalent source point is ambiguous. The horn lengths used (see section II B 2 e) are approximately 70 centimeters in length. Distances measured from transmitter horn mouth to receiver horn mouth may therefore be short by this order of magnitude. Experimental data was arbitrarily corrected by adding 50 centimeters to the mouth to mouth distance. The effect is greatest at the shorter distances. Accurate theoretical calculation of points of signal maxima is likewise most affected at the shorter distances. The points of signal addition are best determined experimentally. It is of importance, however, to estimate phase errors introduced by mislocation of the receiver horn from such points. This mis-location may be due to faulty measurement of the electrical maximum, but of greater interest is the error introduced by motion of horn D in measuring phase. The back-and-forth motion permitted from a maximum signal point may be obtained by differentiating θ_{CD} with respect to the horizontal distance x (appendix B 1). The result of this operation is shown in curve a, figure 10. In general, except for a critical region near 200 centimeters, a motion of 1 centimeter results in less than one degree error. This curve was used to correct the experimental results.

b. Height fluctuation: Horn D, in moving back and forth, may change its height above the water slightly due to a tipped mount. This will effect the phase result. The amount of height fluctuation permitted may be obtained by differentiating θ_{CD} with respect to height h_D (Appendix B 2). The result is shown in curve b figure 10. In general, except at distances less than 200 centimeters, a one millimeter fluctuation will introduce less than one degree error.

c. Vertical alignment: The accuracy of this method depends upon the symmetry of the cross paths. The cross path phases θ_{AD} and θ_{BC} must be alike. For this reason (and because these phases are sensitive to distance as seen in appendix A 3) no motion of the cross path horns is permitted, i.e., horns A and D are fixed while transmitting from A; horns C and B are fixed while transmitting from C. In order that θ_{AD} equal θ_{CB}, r_{AD} must equal r_{CB}. The variation in horizontal distance between pairs of horns may be obtained by differentiating θ_{AD} with respect to x (Appendix B 3). The result is curve c, figure 10.

d. Height differences: From appendix B 4, variations in the average height (as compared with the fluctuating height mentioned above) of horns C and D above horns A and B will affect the phase accuracy. Horns A and B may be assumed to be easily maintained at equal heights above water level. The tolerance in top horn height differences, calculated from the differential of θ_{AD} with respect to h_D is given by curve d, figure 10.

e. Horn construction: In order to minimize side reflections, decrease the required transmitter power, and yet keep to a reasonable horn size, horns with 20 decibels down 30 degrees from the axis were chosen. Design followed directly from reference 2 and resulted in horns 1.5" x 2.5" at the throat, 30" long, and 1.5" x 20" at the mouth. From the above discussion it is evident that the only critical feature of the horn construction is a mouth accurate to within one millimeter. Different internal reflections between various horns are not critical because they are equivalent to constant phase angles, all of which eventually cancel out in data reduction.

f. Propagation path: The lobe pattern of the horns chosen indicates a path approximately one half as wide as long. Readings up to 6000 centimeters (roughly 200 feet) being desired, a path 200 feet long by 100 feet wide is required. Measurements at shorter distances of course require less width of path; conversely, if the available path width is less than 100 feet, proportionally smaller ranges must be used.

3. Electrical tolerances

a. Wavelength: To a very good approximation Norton's curves will shift in distance proportional to the wavelength. From inspection of figure 2b, therefore, a one percent shift in frequency can be tolerated without serious error. As has been shown, phase conditions within the equipment are not important as long as the frequency does not shift so radically as to change conditions during the time of measurement. This wavelength tolerance is in marked contrast to that required in an absolute phase system, both in the amount of variation permitted and in the time during which stability is required.

b. VSWR: The standing wave ratio, both in transmitter and receiver is unimportant except for reasons of increased power received. Therefore, minimum tuning was used, and no attempt made to measure VSWR.

c. Transmitter power: The variation of transmitter output power between the two horns, A and C, is not important. Only relative phase is being measured, not relative amplitude. Consequently, the horn and cable system of horn A need not exactly equal the horn and cable system of C.

d. Water depth: Norton's work assumes an infinitely deep, conducting medium. This condition may be approximated providing reflections from the bottom of the water body are negligible. The problem of wave incidence upon a multi-layered dielectric configuration is very difficult to solve and worse to evaluate numerically. For this particular case, however, a satisfactory guess may be made. The problem of plane wave normal incidence is first solved for an air-water-soil configuration (appendix C and figure 11). Depending upon the exact depth of the water, the bottom reflected wave may diminish or reinforce the surface reflected wave. Figure 12 therefore shows a hatched area as a plot of normal incidence reflection ratio (R) versus the attenuation function $e^{-2\alpha_2 y_0}$. Evidently values of the attenuation function of 0.1 or less should be used. The so-called "skin depth" value of this function (1/e) is unsatisfactory.

The normal incidence solution may now be expanded to include other angles of incidence by comparison with pages 304 and 357 of reference 3. This reference solves a more general problem, inspection of which shows that the exponential attenuation function, instead of being $e^{-2\alpha_2 y_0}$ is actually

$$e^{-2\alpha_2 y_0 \left(\sqrt{\frac{\varepsilon_2}{\varepsilon_2 - \sin^2 \psi_2}} \right)}$$

The dielectric constant of water, ε_2, is 80. The square root expression above, therefore, is close to unity for all angles of incidence, ψ_2. Physically speaking, the waves impinging obliquely are bent very close to the normal due to the high dielectric constant of water.

If a condition corresponding to an attenuation function of 0.1 is considered satisfactory, appendix D shows that about one inch of sea water or about 30 feet of lake water is necessary. Such a depth of lake water is too great for ease of horn stand construction. Sea water is not always available. The dilemma may be resolved by addition of sufficient electrolyte to the water. It was necessary in the actual experiment, for example, to use a pond of fresh water six inches deep, 45 feet wide, and 150 feet long. The required conductivity for the six inch depth (appendix D) is 0.666 mhos per meter. From appendix D, therefore, addition of

$$(0.34)(0.666)(150)(45)(0.5) = 777$$

pounds of stock salt to the pond would achieve the required conductivity and adequately reduce the bottom reflections. In the experiment itself, 1000 pounds of salt was added. Common salt was chosen because it was least in cost.

4. Expected accuracy: From the foregoing considerations accuracies of within 10 degrees should be expected. On an absolute scale this represents an overall accuracy of 1/6000 at 1000 centimeters. Relative to the expected result, the accuracy is within 10 percent. Such accuracy in a propagation experiment is reasonable.

III. DESCRIPTION OF EQUIPMENT AND SITES

A. List of equipment

4 microwave horns made of riveted aluminum sheet (13)*

2 stainless steel and aluminum horn support stands. The receiver stand supports 2 precision millimeter drive screws (13 and 16)

30' RG-8/U cable, type N connectors (13)

1 Hickock audio oscillator (14)

1 Hewlett - Packard square wave generator (14)

1 Microline SX - 11 klystron signal source with 417B klystron (14)

1 Coaxial wavemeter (14)

1 TS 12 AP Standing wave indicator (15)

1 1N21 crystal in coaxial crystal holder (15)

4 Waveguide exciter sections (16)

1 5 kw, portable, 120 v, 60 cycle power supply (Pt. Mugu only)

B. Connections of the equipment

The transmitter consists of the audio oscillator supplying a 25 volt, 1500 cps signal to the square wave generator which in turn modulates the signal generator with a 50 volt, 1500 cps square wave. Square wave reflector voltage modulation of the klystron is necessary to minimize frequency modulation of the microwave output and yet provide a variable amplitude signal

---

* Numbers refer to pertinent figures at the end of text.

which can be amplified conveniently at the receiver. One output connection of the 417 B klystron is modified to a type N connector into which a coaxial line from either horn A or horn C may be plugged. The other 417 B output is connected to the coaxial wavemeter, which serves both to measure wavelength and to afford some tuning action.

The receiver is composed of two horns connected through a coaxial "T" to a crystal mixer, the 1500 cps audio output of which is amplified by the standing wave indicator (high amplification audio amplifier) to drive a milliameter mounted on the face of the indicator. Proper crystal connections and some tuning action are provided by a single stub tuner close to the crystal.

All horns are fed by exciter section waveguides, each having slide fitting probes and two tuning screws. These adjustments provide maximum transmitter output from horns A and C, maximum signal into horn B and, on horn D, provide the "attenuator action" specified in section II B 1.

The stands were designed and built by R.W. Paulson and J.H. Watkins under the specifications outlined in section II B 2. Adjustment screws were provided to level the horns, adjust their heights, and raise and lower the structures to accomodate various water depths. The stands worked well.

C. The Pt. Mugu Lagoon

Several sites were investigated including an ideal casting pond in Oak Grove Park, Pasadena; a trout fishing pond on Rosemead Boulevard, San Gabriel; and Morris Dam Lake, Azusa. For reasons of inadequate depth (without salt -- a requirement of the Pasadena Park Department) or too great a depth for stable operation, these sites were not used. A sea water, controlled-depth (tide gate) lagoon at NAMTC, Pt. Mugu, California seemed to offer ideal conditions with the exception of a soft mud bottom and occasional winds. An alternate site in the lagoon but on the seaward (or uncontrolled level) side of the tide gate was also selected. Both sections of the lagoon provide sufficient area (at least 100 x 200 feet) of sufficiently shallow water (less than 12"). Winds are highest between 1 PM and 6 PM, are lowest in the early morning.

D. Pasadena City College Mirror Pond

This site was chosen as a secondary location rather than as a primary location because of its fresh water content (requiring 777 # of salt) and because of its restricted width (45 feet). Horns sufficiently narrow-beamed to eliminate side reflections for the 150 foot length would be too large to warrant the increased effort and expense of horn and stand construction. Therefore the greatest useable range in this pond is twice 45 or 90 feet. The pond, however, has the advantages of being hard-bottomed, sheltered, and of controlled, uniform depth. Figure 17 shows a view of the pond.

IV. THE EXPERIMENT

A. Procedure

The following procedure was used for each set of readings:

1. The transmitter and receiver stands were placed on the pond bottom and adjusted to an approximate level. The lower horns were adjusted in height as close as possible to the water level without permitting calm water entry. The upper horns were adjusted to 125 centimeters (center of the horn) above water level.

2. The transmitter stand was leveled and so adjusted that the mouths of horns A and C were vertically aligned to within one millimeter.

3. The transmitter was turned on and tuned to 10.00 centimeters wavelength. Microwave energy was directed by coaxial cable to the upper transmitter horn, horn C.

4. The receiver was turned on. Horn D only was used. The received signal was maximized by adjustment of the tuning stubs on exciter sections C and D.

5. With all electrical equipment turned on the receiver system was shifted toward and away from the transmitter to a point of maximum received signal. The receiver stand was leveled and properly adjusted in height. Horn D was moved back and forth along its screw to find the true maximum signal point. The maximum was broad, as predicted. The true maximum point was chosen as the scale reading at which a maximum signal

strength existed at the same amplitude for the same distance in both directions.

6. The distance between the horn C mouth and the horn D mouth was measured with a surveyor's steel tape.

7. With horn D at the maximum point the mouth of horn B was plumb bobbed vertically below the mouth of horn D.

8. The reading on the horn D scale (top zero) and the reading on the horn B scale (bottom zero) were indicated on the data sheet.

9. Horn D (receiver top) was disconnected and horn B (receiver bottom) connected in its place. Tuning stubs on exciter section B were adjusted for maximum received signal. The amplitude was noted. Horn D was then substituted for horn B and de-tuned to yield the same received signal amplitude as had horn B.

10. Both receiver horns were now connected through a coaxial "T" to the crystal detector.

11. With the transmitter still radiating from horn C horn D was moved along its scale to a point of minimum received signal. The meter scale reading was noted (top minimum).

12. Horn D was returned to its zero position.

13. The transmitter was switched to horn A.

14. Horn B was moved to a point of minimum received signal. The meter scale reading was noted (bottom minimum).

15. The bottom scale reading at minimum plus the top zero were subtracted from the top scale reading at minimum plus the bottom zero.

16. The resulting answer in centimeters was multiplied by 36.0 to yield the phase shift.

B. Pt. Mugu Lagoon

Through the cooperation of the range instrumentation section, NAMTC, Pt. Mugu, the Pt. Mugu lagoon and the facilities of the Navy base were made available from 4 May 1950 to 9 May 1950. Unfortunately, at this period a series of very low (minus 1.4 feet) tides resulted in the automatic draining of all water from the inland side of the tide gate (see section III C). All work had been undertaken with the understanding that the normal drainage control action of the tide gate was not to be hampered. Experiments were therefore made at the alternate seaward site. Platform sleds having wooden runners and slanted fore and aft sections were used to move the equipment on the mud bottom. Design was based upon a ten pounds per square foot mud support strength, determined empirically. One of the three sleds may be seen beneath the receiver in figure 13. Difficulty was experienced starting the sleds' motion due to high mud suction. Once started, the sleds were moved easily by one man ashore pulling on two quarter-inch hemp ropes.

The tide condition provided many obstacles to success. Designed for the slow water depth changes of the controlled section of the lagoon, the screw height adjustments on the stands could not compensate for the tide action. The time of high and most stable tide coincided with periods of highest wind. The wind rocked the light weight stands, rippled the water to two inch waves, and chilled the personnel working hip deep in mud and water. The waves bounced the lower horns and often partly filled them with water, producing a wildly-oscillating received signal. Readings obtained were meaningless. The Norton phase shift could not be checked but the amplitude relationships of section II B 1 were roughly confirmed, the basic technique proved valid, and the electrical equipment tested under rugged conditions.

It is suggested, nonetheless, that the Pt. Mugu lagoon not be discarded in consideration of further work. The controlled section, in particular, may well be satisfactory in the early morning hours when little wind is present. The electrical conductivity of this fresh-water-fed section is between one quarter and one half that of sea water. A water depth of two to four inches is readily achieved under proper conditions. Mud sledding, while uncomfortable, is not impossible.

C. The Pasadena City College Mirror Pond

With failure on the Pt. Mugu attempt, work was initiated immediately to modify the equipment for use in the PCC Mirror Pond. The sleds were discarded and all cables were cleaned of brine. One half ton of #1 grade stock salt was dissolved in the pond. By 15 May 1950 the equipment was ready and on the site.

A difficulty first observed in the Pt. Mugu attempt tended to confuse the location of the maximum E_{CD} signal. The accuracy of the experiment, it has been shown, depends upon reasonably accurate location of these maxima. Apparently due to the phase properties of the horn lobe patterns, a smooth variation of signal strength with distance was not observed. The points of true maximum signal were preceded and followed by a series of smaller maxima superimposed on the basic variation. Bottom reflections may have been the cause, but this is doubtful. In the Pt. Mugu experiment the water was over six inches deep at all points, more than enough to attenuate the bottom reflected wave below detection. Confusion was greater at the shorter distances. Experimentally it was observed that even a shallow film of water in either the lower transmitter or receiver exciter sections greatly attenuated the received signal. Presumably a phase shift due to the water film occurred as well. From the foregoing theoretical discussion (section II B 1 and section II B 3 b) these phase shifts are not important unless they change during a set of readings. Motions of the horns during a set of readings (other than the known motion along the millimeter screws) caused by tipping of the stands while turning the screws distorted the readings unless care was taken to make all measurements slowly.

With the exception of these unexpected annoyances, the procedure was followed easily. Each set of readings took approximately one half hour. The set up time required was three hours.

V. RESULTS

Readings were taken at six distances at which E_{CD} was a maximum. The data is given in appendix E. The readings were then corrected according to figure 10 (tolerances curve a). Fifty centimeters was arbitrarily added to each measured distance (horn mouth to horn mouth) in order that the results might be plotted on a source-to-source distance scale. Appendix F gives the corrected values. Figure 18 shows the comparison with theory.

Of the six readings, four are within the expected accuracy limits of $\pm$ 10 degrees. It is believed that the experimental points at 298 and 493 centimeters are erroneous. The magnitude and character of the variation suggests a consistent mistake in procedure -- probably omission of step 12. Note that a line drawn between these two points will approximate the slope though not the magnitude of the Norton curve.

It appears likely that these data confirm Norton's theory, if only by inference. Obviously all measured phase angles might be in error by multiples of 360 degrees. If this were the case, however, it is improbable that the resulting total phase angles would obey the same law of behavior as Norton predicted. In other words, the points should be either at random, of different order of magnitude (greater than 180 degrees occasionally), or of different slope. There remains the question whether or not all antennas will generate this Norton wave. This experiment seems to show that given sufficient generating area such a wave does travel along a conducting surface.

VI. SUGGESTIONS FOR FURTHER WORK

The above results yield a good check on the technique proposed and provide a preliminary check on the Norton phase shift. Further work undoubtedly is indicated, particularly at the shorter distances. Small horns mounted on nearly reflection-free stands should be used. No unessential transmitting and receiving equipment or other extraneous reflectors should be present within the beams of the horns. The horn motion concept for measuring phase is recommended for simplicity, although a precision measurement undoubtedly should use a calibrated line stretcher in a unity VSWR system. Research personnel continuing this work should exercise extreme safety precautions. Standing in six inches of water adjusting electrical equipment is dangerous. All chasses of electrical equipment should be connected together and grounded to the water.

The basic technique proposed here may be used to check other theoretical phase conditions than the phase characteristics of 3000 megacycles/sec. over water. Different ground conditions and different propagation frequencies can provide information of other "B" curves and on other ranges of "P". The method is equally applicable for the study of the phase distortion of waves propagated over ridges. The free space criterion is always met by using points of maximum E_{CD}.

APPENDIX A

1. Calculation of E_{AB} (fresh water case)

Equation 1) of the text may be used with the following modifications:

$$\cos \Psi_1 = \cos \Psi_{AB} \cong 1.00$$

$$\cos \Psi_2 = \cos' \Psi_{AB} \cong 1.00$$

$$h_A = h_B = 2.5 \text{ cm} \ll r$$

$$R = \frac{\sin' \Psi_{AB} - \varepsilon^{-\frac{1}{2}}}{\sin' \psi_{AB} + \varepsilon^{-\frac{1}{2}}} = \frac{5 - 0.1118\ x}{5 + 0.1118\ x}$$

$$P = \frac{4\ p}{(1 - R)^2} = 0.315\ \frac{(5 + 0.1118\ x)^2}{x}$$

$$r_1 - r_2 \cong 2\ h_A^2 / x$$

$$B = b = 90^{\circ}$$

Therefore,

1) $$E_{AB} = E_{AB}\ e^{i\ \Theta_{AB}}$$

$$= \frac{E_o}{x}\ e^{i\ 2\pi x/\lambda} \left[\frac{5 - 0.1118\ x}{5 + 0.1118\ x} \cos\left(\frac{450}{x}\right)^{\circ} + 1 + f(P,B)\ (1 - R) \cos\left(\phi + \frac{450}{x}\right)^{\circ} \right]$$

$$+ i\ \frac{E_o}{x}\ e^{i\ 2\pi x/\lambda} \left[\frac{5 - 0.1118\ x}{5 + 0.1118\ x} \sin\left[\frac{450}{x}\right]^{\circ} + f\ (P,B)\ (1 - R) \sin\left(\phi + \frac{450}{x}\right)^{\circ} \right]$$

Let $K = \frac{E_o}{x} e^{i\ 2\pi x/\lambda}$, evaluate f(P,B) and from figures 2a and 2b respectively; and substitute numerical values, From which the following table results.

d	$\left.\frac{E_{AB}}{K}\right\|_{real}$	$\left.\frac{E_{AB}}{K}\right\|_{imag.}$	θ_{AB}
67.5	1.0595	0.3115	16.4°
201.3	0.616	0.3417	29.1
522.5	0.285	0.2728	43.8
1105	0.128	0.1758	54.0
1788	0.717	0.1203	58.8
3000	0.387	0.0785	63.5

θ_{AB} is plotted in figure 5.

2. Calculation of E_{AB} (salt water case)

In case of appreciable conductivity the phase angle of R is not a simple 0° - 180°, but is given instead by figure 2c. Equation 1 then becomes

$$\frac{E}{K} = \left[|R| \cos\left(\frac{450}{X} + \phi_R\right)^\circ + 1 + f(P,B)(|1-R|)\cos\left(\phi + \frac{450}{X} + \phi_{1-R}\right)^\circ \right]$$
$$+ i\left[|R| \sin\left(\frac{450}{X} + \phi_R\right)^\circ + f(P,B)(|1-R|) \sin\left(\phi + \frac{450}{X} + \phi_{1-R}\right)^\circ \right]$$

and $Pe^{iB} = \frac{4p}{(1-R)^2}$; i.e., $B = b + 2\phi_{1-R}$

(b for salt water at 3000 mc = 69.4°),

from which, upon substitution of numerical values, we obtain the following table.

d	$\left.\frac{E_{AB}}{K}\right\|$ real	$\left.\frac{E_{AB}}{K}\right\|$ imag.	θ_{AB}	$\left\|\frac{E_{AB}}{K}\right\|$
67.3	1.153	.5375	25°	1.272
201.3	.5725	.4757	39.5°	.745
522.5	.2057	.3631	60.6°	.417
1105	.0558	.2418	77°	.248
1788	.0296	.1378	78°	.1414
3000	.0119	.0916	82.6°	.0925
6000	.00680	.04076	83.5°	.0413

θ_{AB} is plotted in figure 5.

$\left|\frac{E_{AB}}{K}\right|$ is plotted in figure 6 as E_{AB}.

3. Calculation of E_{AD} (fresh water case).

$$E = \frac{E_0}{x}\left[\cos^3\psi_{AD}\, e^{i\frac{2\pi r_{AD}}{\lambda}} + R\cos^3\psi'_{AD}\, e^{i\frac{2\pi r'_{AD}}{\lambda}} + (1-R)f(P,B)\cos^3\psi'_{AD}\, e^{i\left(\frac{2\pi r'_{AD}}{\lambda}+\phi\right)}\right]$$

$$\psi_{AD} \cong \psi'_{AD} \qquad \cos\psi_{AD} \cong \frac{x}{\sqrt{x^2+(125)^2}}$$

$$\frac{E}{K} = \cos^3\psi_{AD}\, e^{i\left[\frac{2\pi}{\lambda}(r'_{AD}-x)\right]}\left[e^{i\frac{2\pi}{\lambda}(r_{AD}-r'_{AD})} + R + \frac{(1-R)f(P,B)e^{i\phi}}{\cos\psi_{AD}}\right]$$

where $\quad r_{AD} - r'_{AD} \cong \dfrac{5}{\left[1 + (x/125)^2\right]^{1/2}}$

$$R = \frac{\sin\psi_2 - 0.1118}{\sin\psi_2 + 0.1118} \qquad \psi_2 \equiv \psi'_{AD}$$

$$P = 0.315\ x_{CM}\frac{(\sin\psi_2 + 0.1118)^2}{\cos\psi_{AD}}$$

$B = b = 90^{\circ}$

from which numerical evaluation yields the table below.

d	θ_{AD}	$\lvert E_{AD}/K \rvert$
50	3229.3	0.0148
100	2322.2	0.148
300	986	1.025
500	573	1.191
1000	384	.993
2100	168	.720
4500	80.2	.417

$\lvert E_{AD}/K \rvert$ has been plotted in figure 6 as E_{AD}. Note the rapidly changing θ_{AD}.

4. Calculation of E_{CD} (fresh water case)

Assume $h_C \cong h_D = 125$ CM, $\psi_{CD} = 0$, only points of amplitude addition valid, and that K is as given previously.

$$\frac{E_{CD}}{K} = \left[1 + R\cos^3\psi'_{CD} + f(P,B)(1-R)\cos\phi\right] + j\left[f(P,B)(1-R)\sin\phi\right]$$

for $\sin\psi'_{CD} < 0.1118$.

$$\frac{E_{CD}}{K} = \left[1 + |R|\cos\psi'_{CD} - f(P,B)(1+|R|)\cos\phi\right] - j\left[f(P,B)(1+|R|)\sin\phi\right]$$

for $\sin\psi'_{CD} > 0.1118$.

$$R = \frac{\sin\psi'_{CD} - 0.1118}{\sin\psi'_{CD} + 0.1118}$$ is a good approximation.

Therefore

$$P = 0.315 \times \frac{(\sin \psi'_{CD} + 0.1118)}{\cos \psi'_{CD}}$$

$$B = b = 90^\circ$$

from which a numerical evaluation yields the following table.

d	θ_{CD}	$\left\lvert \frac{E_{CD}}{K} \right\rvert$
50	9	1.039
100	0	1.1775
300	0	1.446
500	0	1.369
1000	0	1.156
2100	0	1.378
4500	0	1.630
6272	$-1^\circ 14''$*	1.706

$\left\lvert \frac{E_{CD}}{K} \right\rvert$, good only at points of amplitude addition, has been plotted as E_{CD} in figure 6. The Norton effect at $h_C = h_D \doteq 125$ CM is negligible.

*Norton Contribution

APPENDIX B

1. Tolerance permitted in motion of horn D from maximum amplitude points. Transmitting from horn C

$$\Theta_{CD} \cong \tan^{-1}\left[R \cos^3 \psi'_{CD} \sin \frac{2\pi}{\lambda} \left(r'_{CD} - x\right)\right]$$

$$\frac{d\Theta_{CD}}{dx} = \frac{\cos^2\Theta_{CD}}{1 + R \cos^3\psi'_{CD}} \; R \cos^3\psi'_{CD} \left[\frac{2\pi}{\lambda} \left(\cos\psi'_{CD} - 1\right)\right]$$

$$\left.\frac{d\Theta_{CD}}{dx}\right|_{\substack{\Theta_{CD} = n\pi \\ \text{for max}}} = 0.628 \; \frac{R \cos^3 \psi'_{CD}}{1 + R \cos^3 \psi'_{CD}} \left(\cos \psi'_{CD} - 1\right) \text{radians/cm},$$

or Δx in centimeters for 1° error near $\Theta_{CD} = n\pi$ is given by

$$\Delta x_{1^\circ} = 0.0277 \left[\frac{1 + R \cos^3 \psi'_{CD}}{R \cos^3 \psi'_{CD}}\right] \frac{1}{\cos \psi'_{CD} - 1} \; .$$

Δx_{1° is plotted in figure 10 as curve a.

2. Tolerance permitted in vertical height of horns C and D from 125 CM of water surface

$$\Theta_{CD} \cong \tan^{-1}\left[R \cos^3 \psi'_{CD} \sin \frac{2\pi}{\lambda} \left(r'_{CD} - x\right)\right]$$

$$\left.\frac{d\Theta_{CD}}{dh}\right|_{\Theta_{CD} = n\pi} = \frac{8\pi}{\lambda} \; \frac{R \cos^3\psi'_{CD} \sin\psi'_{CD}}{1 + R \cos^3\psi'_{CD}} \quad \text{radians/cm} \quad ,$$

or Δh in millimeters for 1° error near $\Theta_{CD} = n\pi$ is given by

$$\Delta h_{1^\circ} = 0.0693 \; \frac{1 + \cos^3 \psi'_{CD}}{R \cos^3\psi'_{CD} \sin\psi'_{CD}}$$

Δh_{1° is plotted as curve b in figure 10.

3. Tolerance in vertical alignments of pairs of horns

$$\theta_{\substack{AD\\CB}} = \mathrm{ARG}\left[K \quad e^{i\frac{2\pi}{\lambda}(r'_{AD} - X)} \left(1 + R e^{i\frac{2\pi}{\lambda}(r'_{AD} - r_{AD})} \right) \right]$$

$$\cong \frac{2\pi}{\lambda} \; (r'_{AD} - X) \quad \text{radians}$$

$$\frac{d\,\theta_{AD}}{d\,x} = \frac{2\pi}{\lambda} \left\{ \frac{x}{[x^2 + (h_C - h_A)^2]^{\frac{1}{2}}} - 1 \right\} \cong \frac{2\pi}{\lambda} (\cos \psi'_{CD} - 1)$$

radians/cm

or ΔX in millimeters for a 1° error is given by

$$\Delta X = \frac{100}{360 \; (\cos \psi'_{CD} - 1)}$$

which is plotted as curve c on figure 10.

4. Tolerance in vertical height of horn D as compared to horn C

$$\theta_{AD} \cong \frac{2\pi}{\lambda} \; (r'_{AD} - X) \text{ radians}$$

$$\frac{d\theta_{AD}}{dh} = \frac{2\pi}{\lambda} \frac{(h_C - h_A)}{[x^2 + (h_C - h_A)^2]^{\frac{1}{2}}} \cong \frac{2\pi}{\lambda} \sin \psi'_{CD} \text{ radians/cm}$$

or Δh in millimeters for a 1° error is given by

$$\Delta h = \frac{100}{360 \; \sin \psi'_{CD}}$$

which is plotted as curve d in figure 10.

APPENDIX C

From figure 11 the boundary conditions may be written as

$$\text{at } y = y_0 \begin{cases} E_1 + E_1' = E_2 + E_2' \\ E_1 - E_1' = \sqrt{\frac{\varepsilon_1}{\varepsilon_2}}\,(E_2 - E_2') \end{cases} \quad \text{at } y = 0 \begin{cases} E_2 + E_2' = E_3 \\ E_2 - E_2' = \sqrt{\frac{\varepsilon_2}{\varepsilon_3}}\,E_3 \end{cases}$$

where

$$\left.\begin{aligned} E_1 &= A\,e^{-j\beta_1 y} \\ E_1' &= B\,e^{j\beta_1 y} \end{aligned}\right\} \quad \beta_1 = \frac{2\pi}{\lambda_0} \qquad \alpha_1 = 0 \qquad \lambda_0 = 10 \text{ cm}$$

$$\left.\begin{aligned} E_2 &= C\,e^{-j\beta_2 y - \alpha_2 y} \\ E_2' &= D\,e^{j\beta_2 y + \alpha_2 y} \end{aligned}\right\} \quad \beta_2 = \frac{2\pi}{\lambda_0}\sqrt{\frac{\varepsilon_2}{\varepsilon_0}} \qquad \alpha_2 = \frac{\pi}{\lambda}\frac{\sigma}{\omega}\sqrt{\frac{\varepsilon_0}{\varepsilon_2}} = 0.105\,\sigma_2 \,\frac{\text{mhos}}{\text{meter}}$$

$$\varepsilon_2 = 80\,\varepsilon_0$$

$$\left.\begin{aligned} E_3 &= F\,e^{j\beta_3 y + \alpha_3 y} \\ E_3' &= 0 \end{aligned}\right\} \quad \beta_3 = \frac{2\pi}{\lambda_0}\sqrt{\frac{\varepsilon_3}{\varepsilon_0}} \qquad \varepsilon_3 = 3\,\varepsilon_0$$

$$\text{and} \quad \alpha_3 = 0.105\,\sigma_3\sqrt{\frac{\varepsilon_2}{\varepsilon_3}}$$

Note that due to the high dielectric constant of water the "skin depth" function at these frequencies is independent of the frequency. Substitution of numerical values yields

$$R = \frac{B}{A} = \frac{0.8882 - 0.755\,e^{j2\beta_2 y_0 - 2\alpha_2 y_0}}{1.1118 - 0.595\,e^{j2\beta_2 y_0 - 2\alpha_2 y_0}}$$

which is an oscillating function of envelopes

$$R_+ = \frac{0.8882 + 0.755\,e^{-2\alpha_2 y_0}}{1.1118 + 0.595\,e^{-2\alpha_2 y_0}}$$

and

$$R_- = \frac{0.8882 - 0.755\,e^{-2\alpha_2 y_0}}{1.1118 - 0.595\,e^{-2\alpha_2 y_0}}$$

This result is not frequency dependent in the frequency range of interest. The two equations above are plotted in figure 12 as functions of $e^{-2\alpha_2 y_0} = e^{-0.21\,y_0}$ where σ is in mhos/meter and y_0 is in centimeters.

APPENDIX D

1. Conductivities required to yield an attenuation function of 1/10 for specified water depths y_o.

y_oCM	σ Mhos/meter	Remarks
2	5	sea water, about 1" deep
5	2	
10	1	
15	0.666	about 6" deep
20	0.500	
1000	10^{-2}	lake water, about 30 feet

2. Pounds of electrolyte per cubic foot of water to yield a given conductivity (σ in mhos/meter)

Substance	lbs/cu.ft.
NaCl	0.34 σ
$\frac{1}{2}CuSO_4$	0.456 σ
NH_4Cl	0.365 σ
NH_4NO_3	0.397 σ

Data calculated from International Critical Tables.

APPENDIX E

Distance (cm)	Top Zero (cm)	Bot.Zero (cm)	Top Min. (cm)	Bot. Min. (cm)	Norton (cm)	Norton degrees
211	21.00	22.04	16.92	16.45	1.51	54
298	26.00	27.06	31.82	29.90	2.98	108
493	29.00	29.42	26.80	30.62	3.40	122
619	15.00	14.82	21.4	22.6	1.38	50
1040	25.00	24.25	25.6	26.8	1.95	70
2026	27.00	28.65	23.6	27.0	1.75	63

Readings decrease as horns moved toward transmitter.

APPENDIX F

Distance	Norton Degrees
261	48
348	114
543	119
669	51
1090	70
2076	63

REFERENCES

1. Norton, K.A., The calculation of ground wave field intensities over a finitely conducting earth, Proc. of the IRE, Dec. 1941 Vol. 29 pages 623 through 638.

2. Terman, F.E., Radio Engineer's Handbook, McGraw-Hill Book Co., New York, 1943.

3. Leaderman, H. and Turner, L.A., Radar Scanners and Radomes, MIT Radiation Laboratory Series Volume 26.

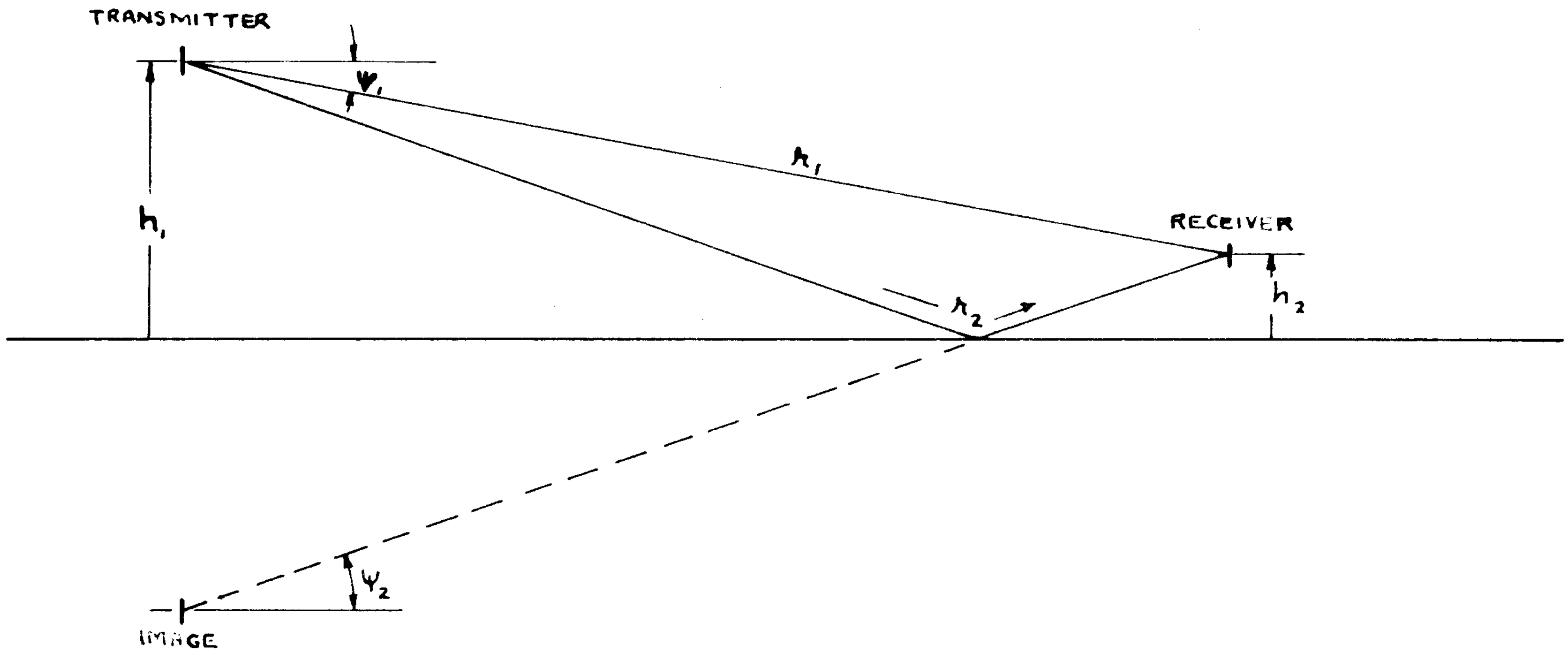

FIGURE 1 NORTON'S ANTENNA CONFIGURATION

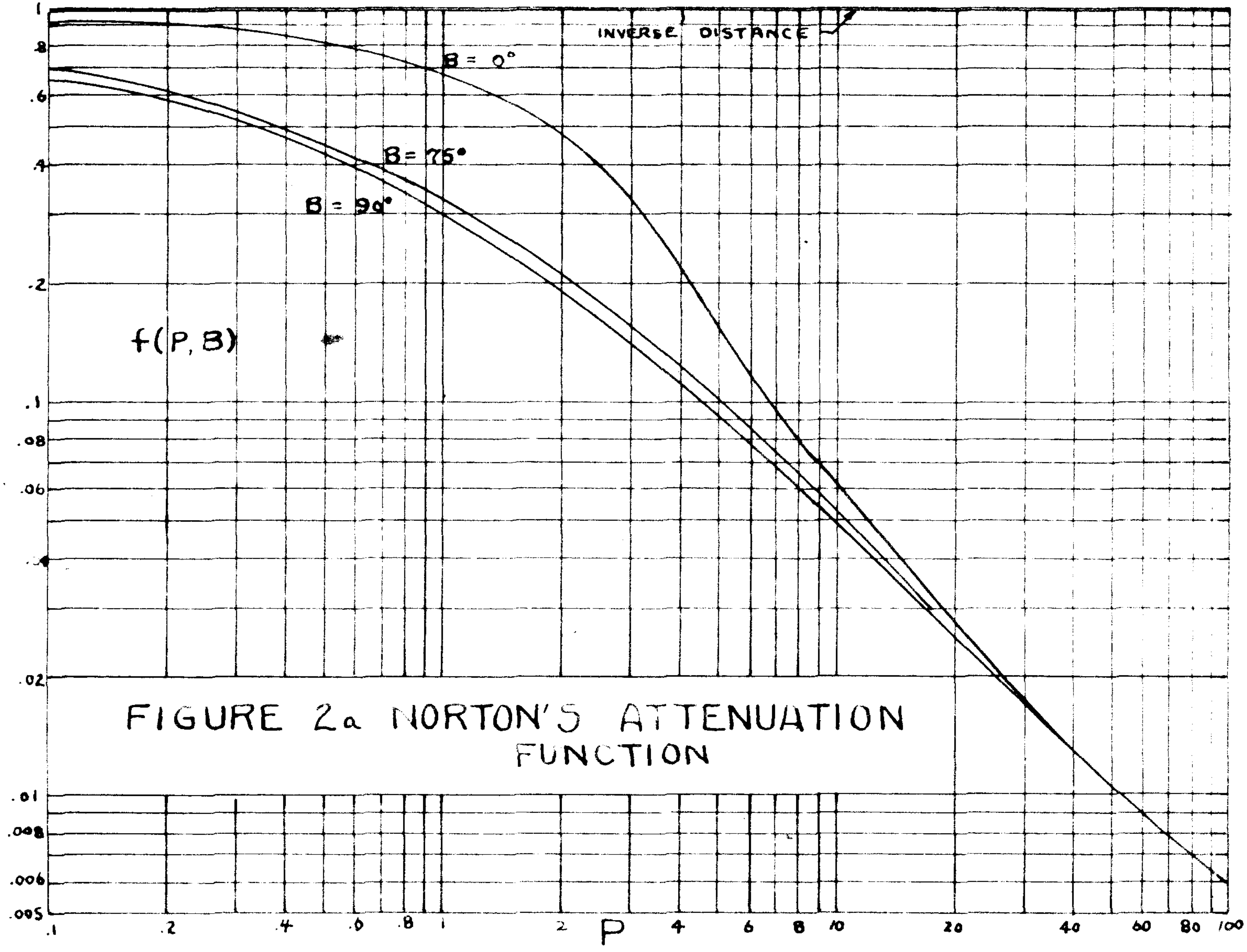

FIGURE 2a NORTON'S ATTENUATION FUNCTION

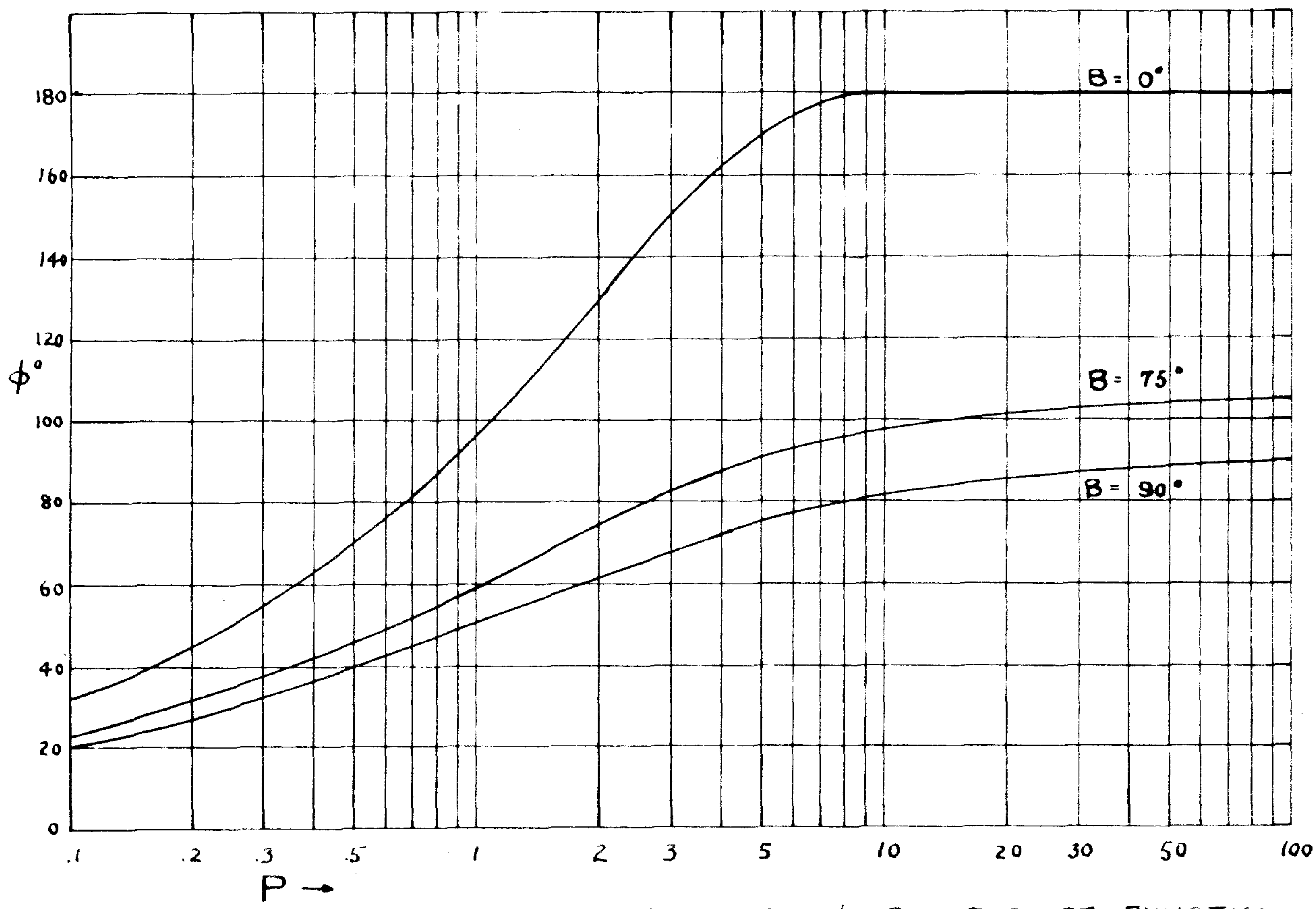

FIGURE 2b NORTON'S PHASE SHIFT FUNCTION

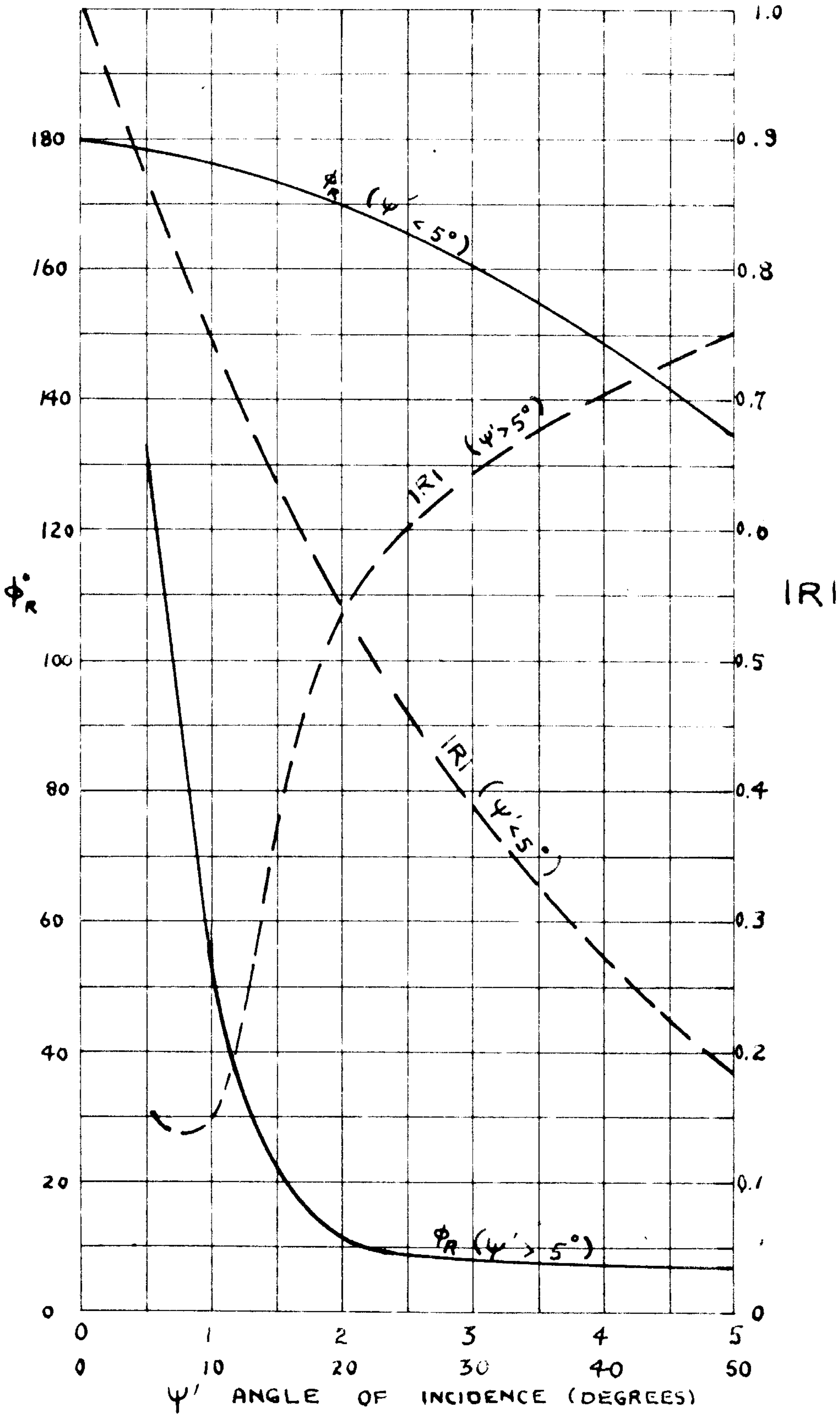

FIGURE 2c REFLECTION COEFFICIENT OF SEA WATER AT 3000 MEGACYCLES/SEC.

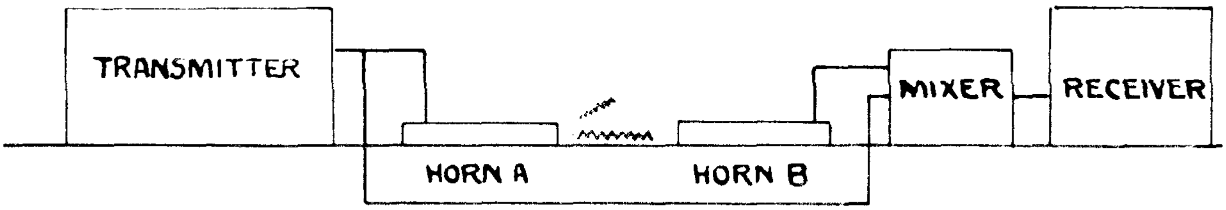

FIGURE 3 METHOD 1

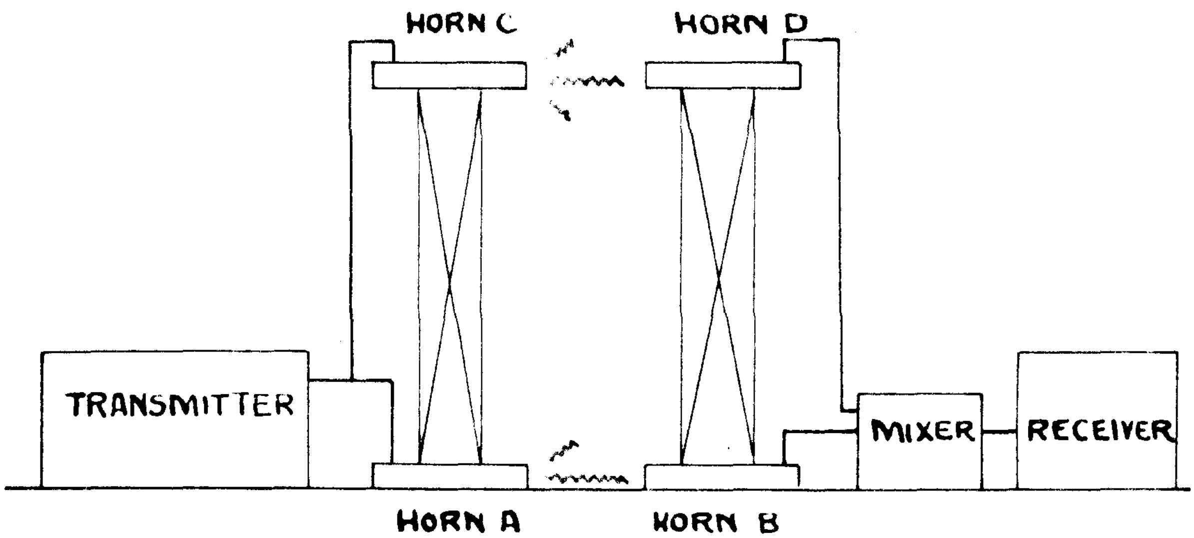

FIGURE 4 METHOD 2

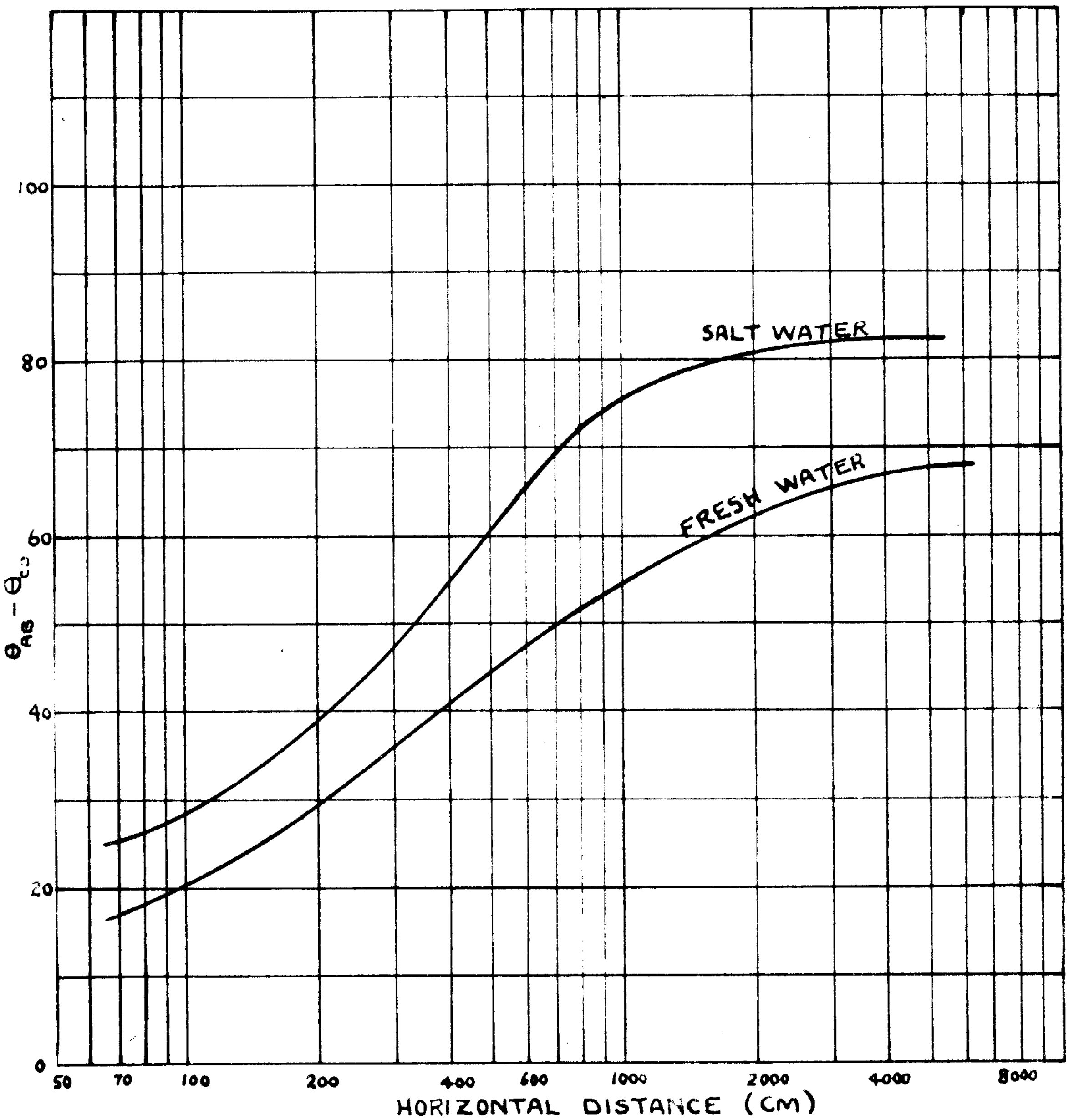

FIGURE 5 PREDICTED RESULTS

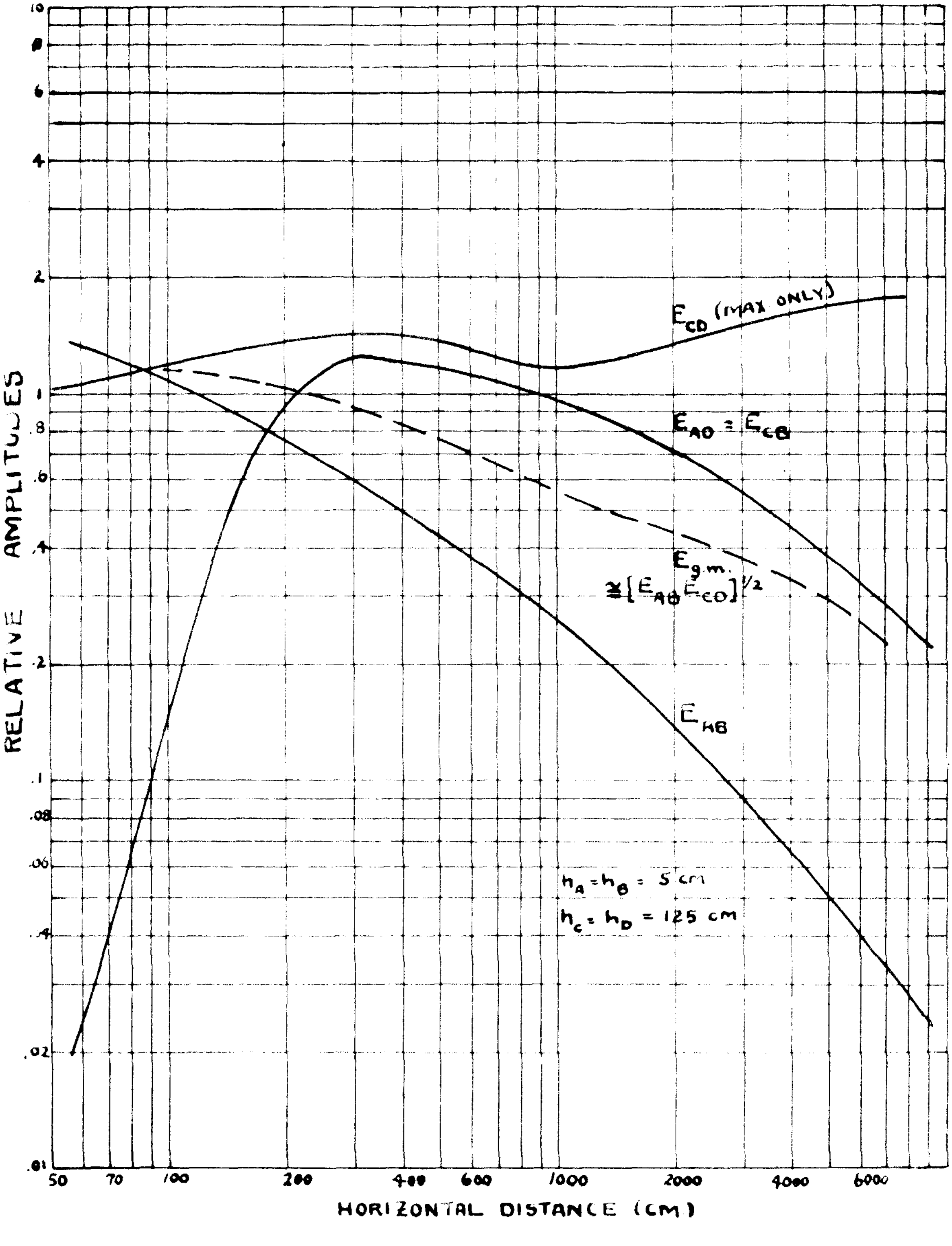

FIGURE 6 RELATIVE AMPLITUDES OF RECEIVED SIGNALS

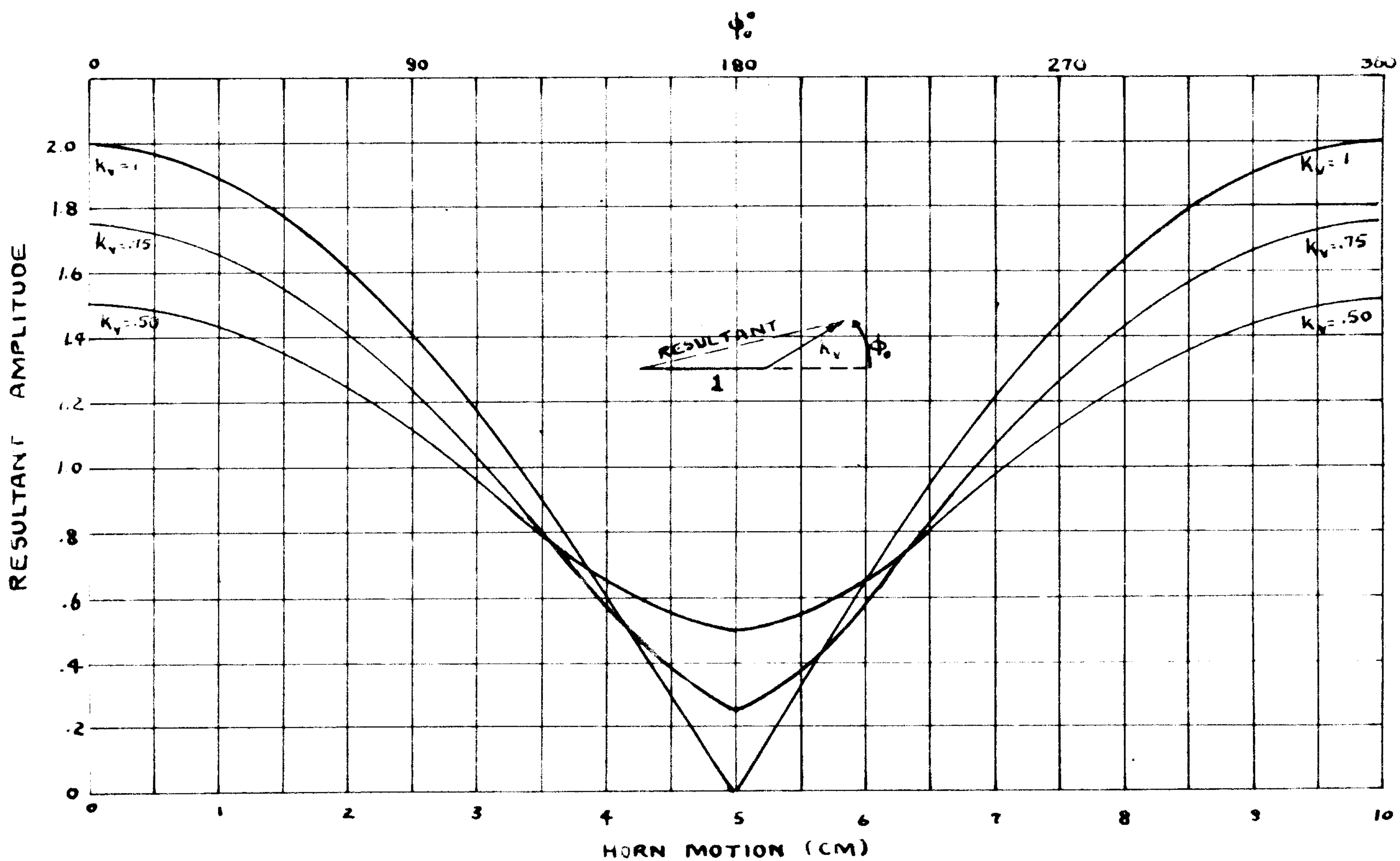

FIGURE 7 RESULTANT OF TWO VECTORS

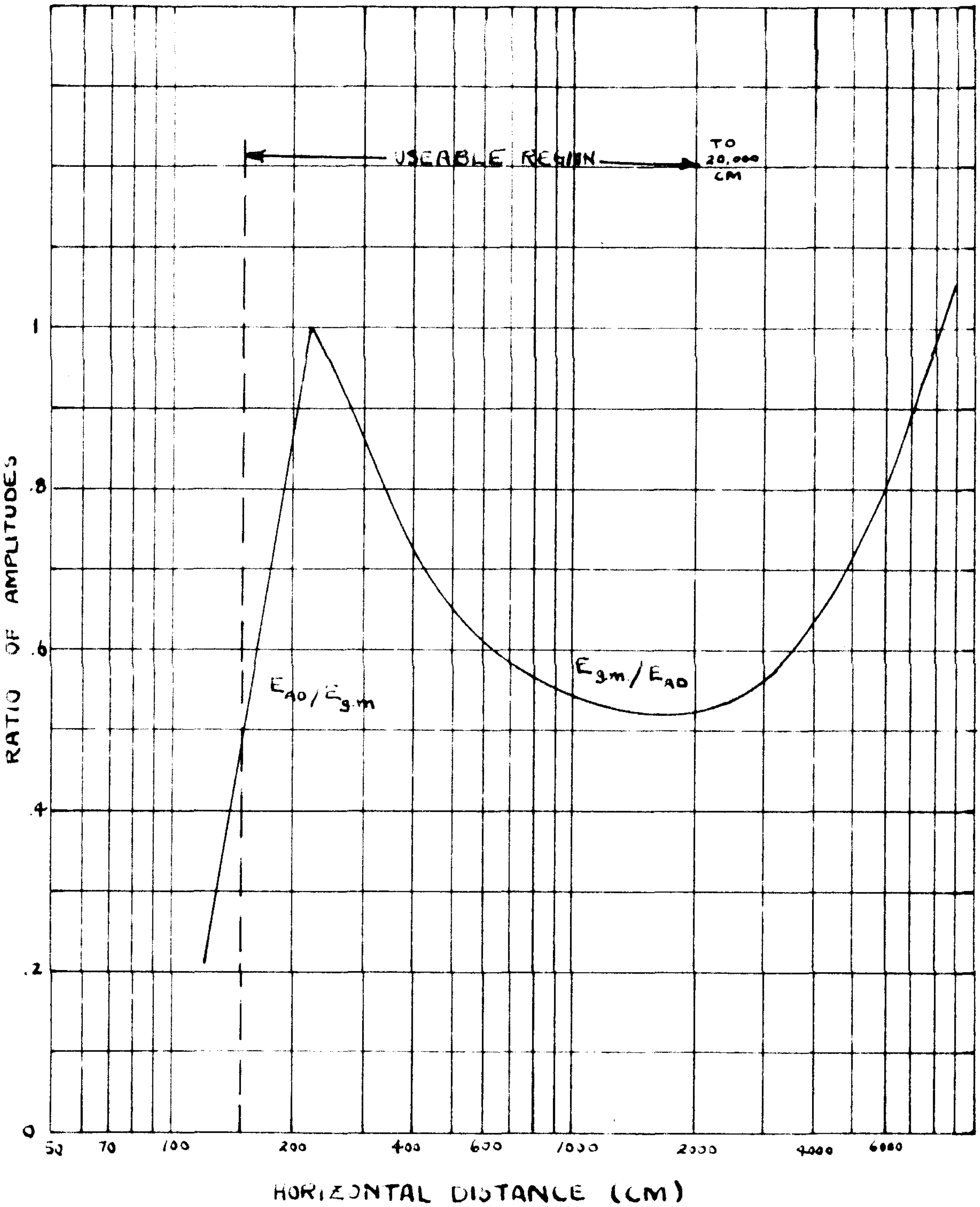

FIGURE 8 USEABLE RANGE ON RELATIVE AMPLITUDE CONSIDERATIONS

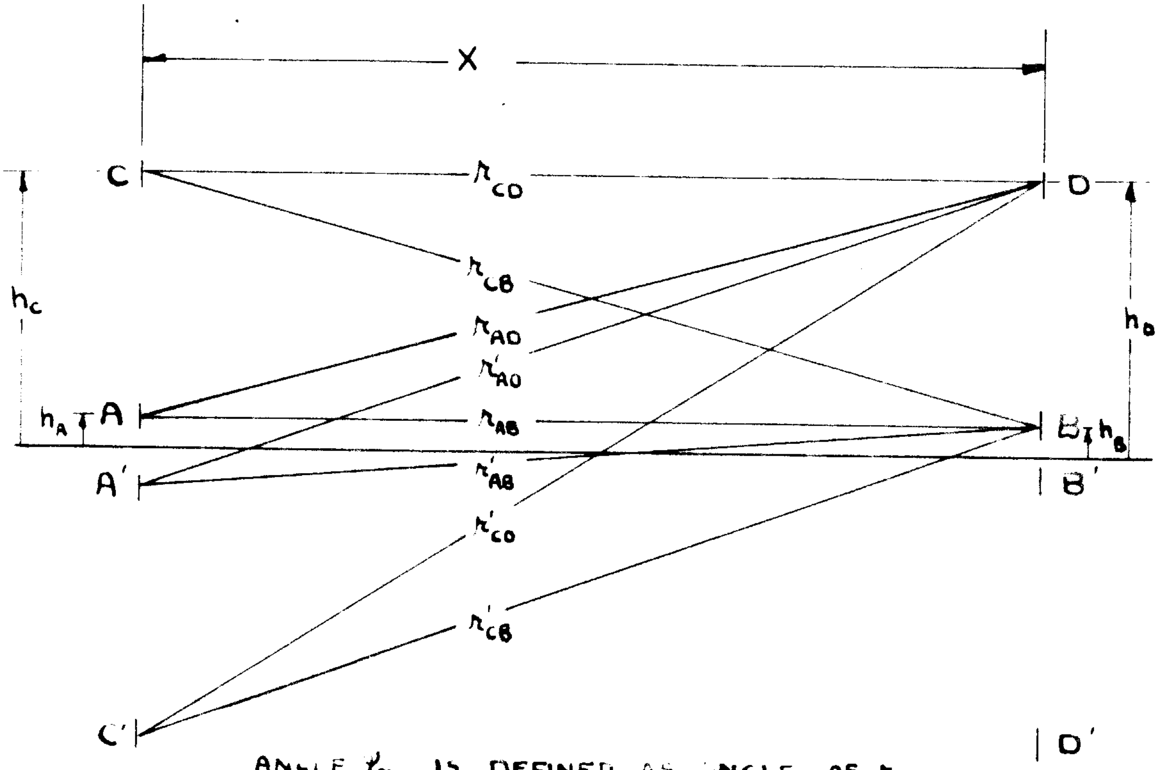

ANGLE ψ_{MN} IS DEFINED AS ANGLE OF r_{MN} WITH HORIZONTAL

FIGURE 9 HORN CONFIGURATION

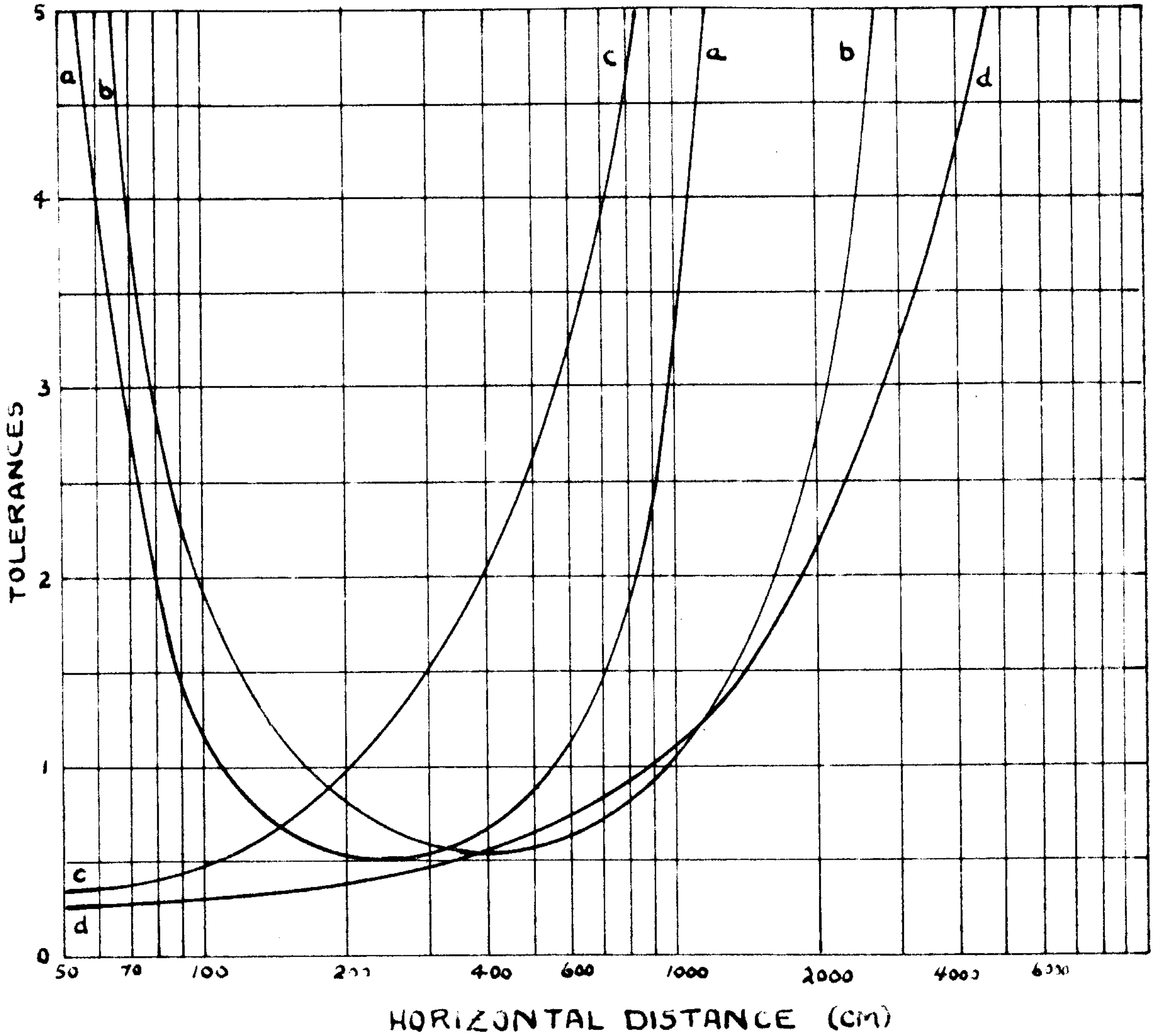

a. Error permitted in distance measurement to E_{CD} maximum point for one degree error (cm)

b. Fluctuation permitted in horn D height during measurement for one degree error (mm)

c. Error permitted in vertical alignments of pairs of horns for one degree error (mm)

d. Error permitted in vertical height difference between pairs of horns for one degree error (mm)

Notes: Motion apart introduces negative phase error

Curves a and b apply only to points of maximum E_{CD}

FIGURE 10 TOLERANCES

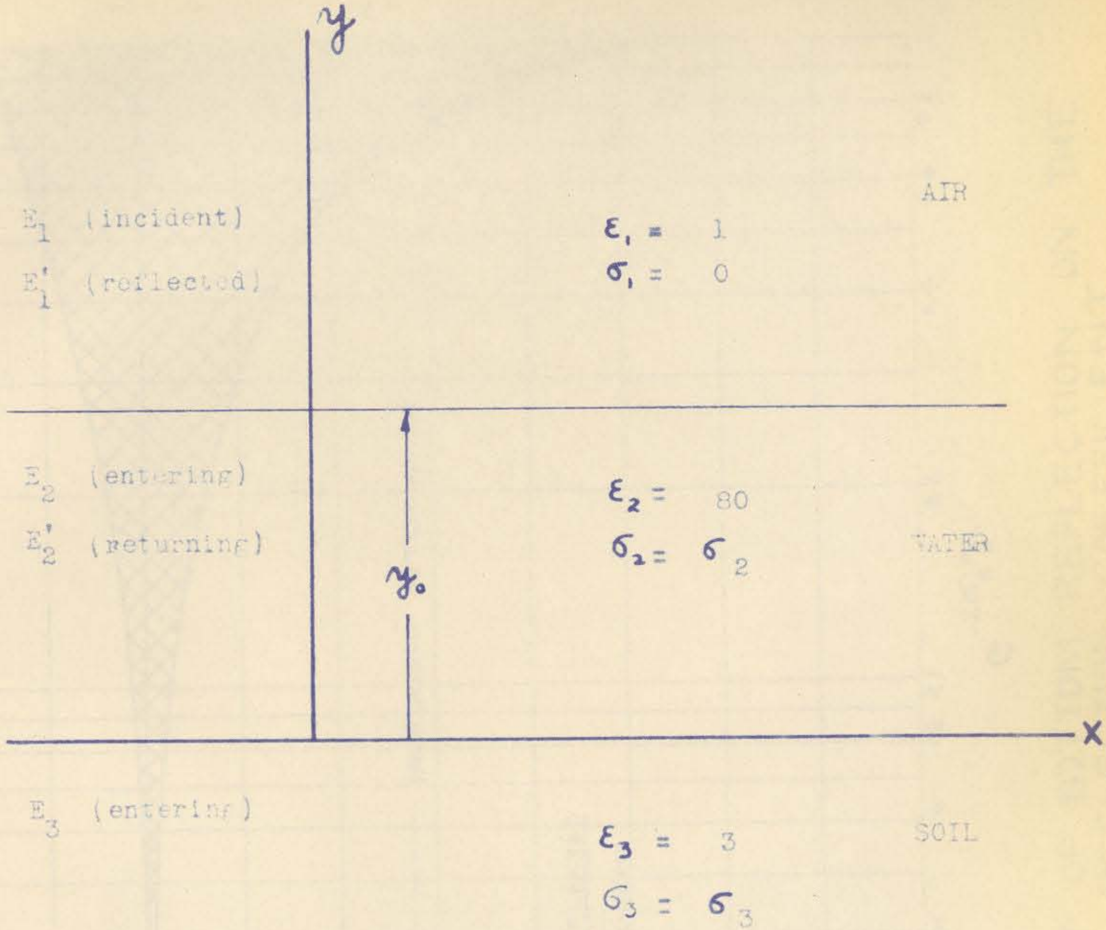

FIGURE 11 NORMAL INCIDENCE CONFIGURATION

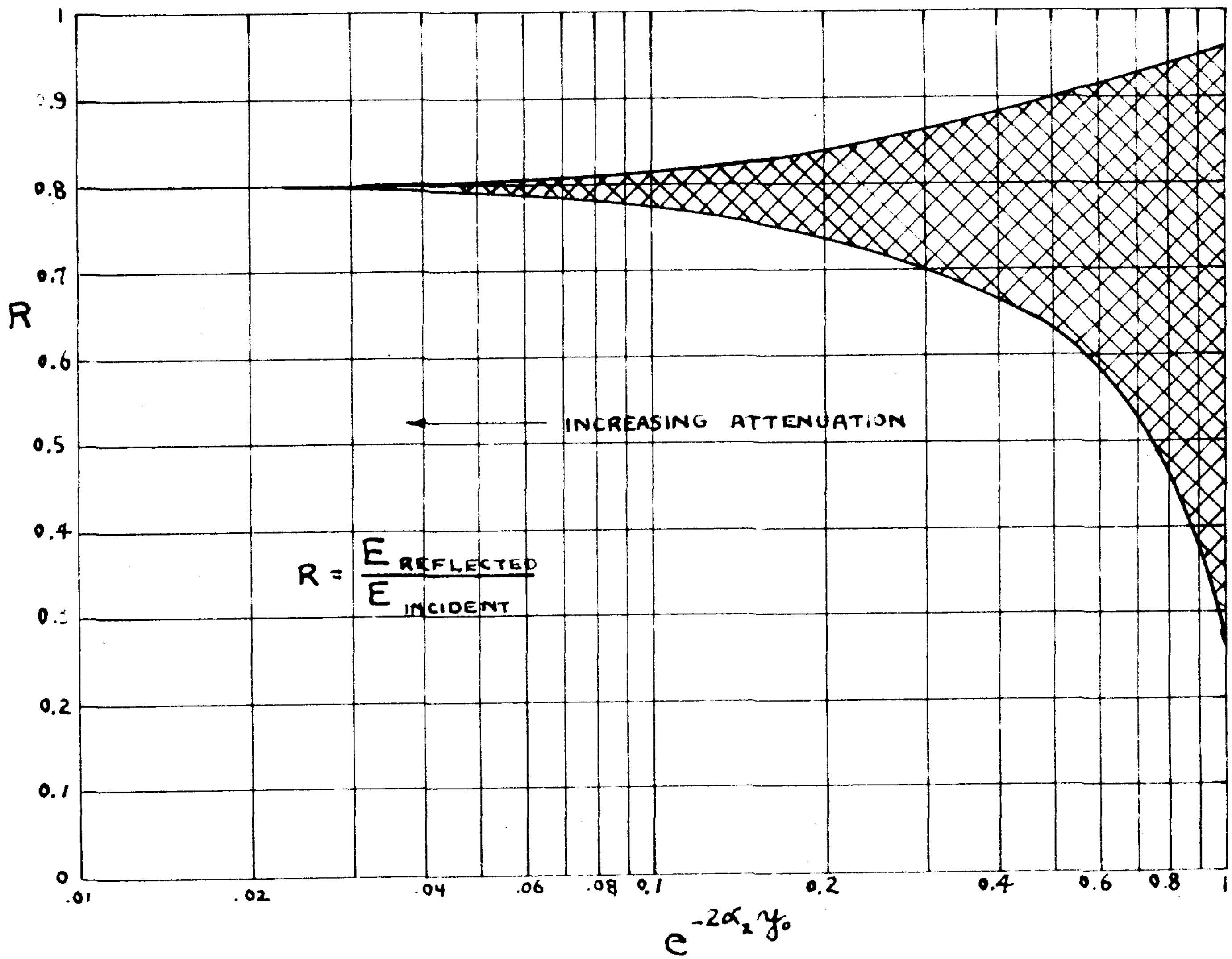

FIGURE 12 EFFECT OF BOTTOM REFLECTION ON THE SURFACE REFLECTION COEFFICIENT

Figure 13 Overall View of Equipment

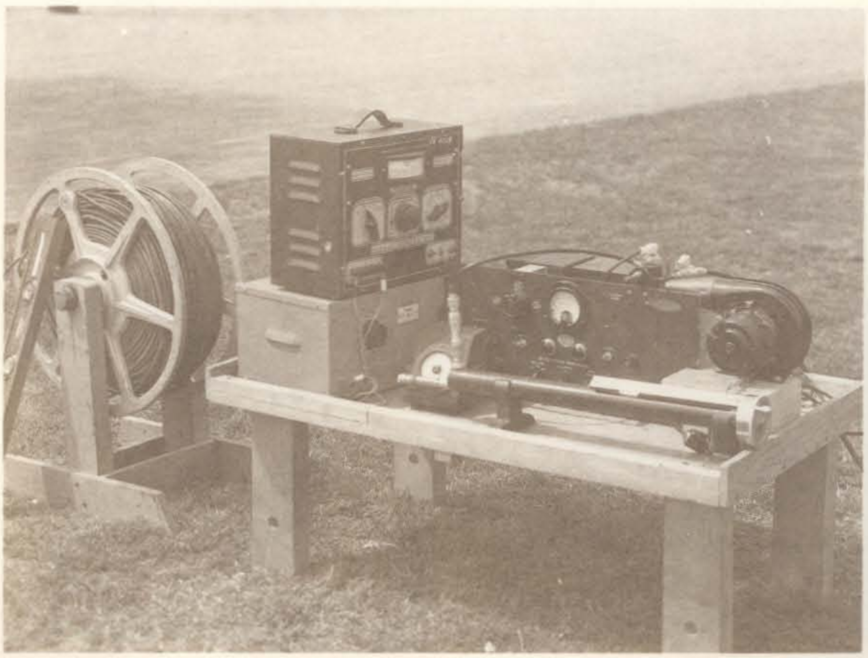

Figure 14 View of Transmitter

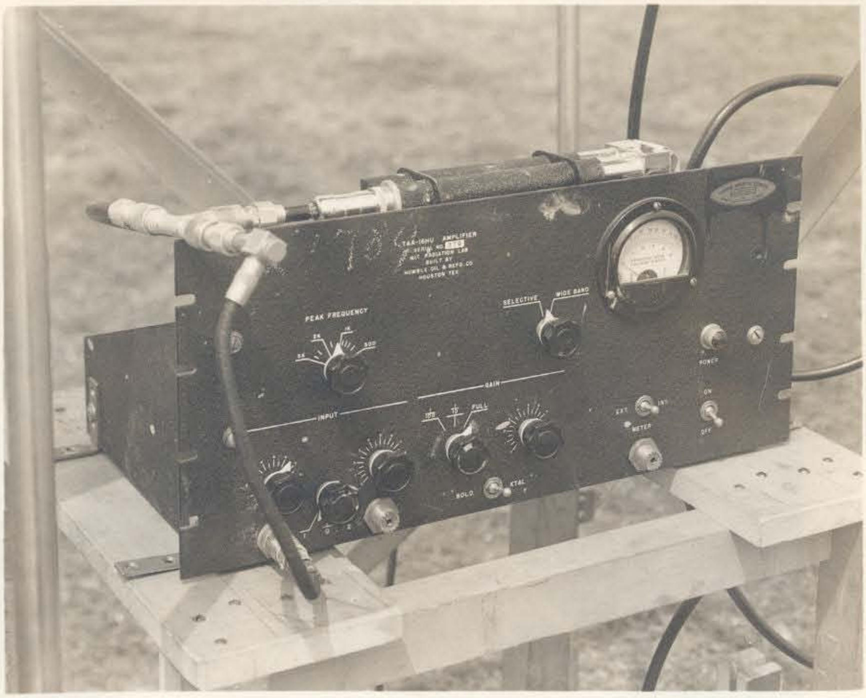

Figure 15 View of Receiver

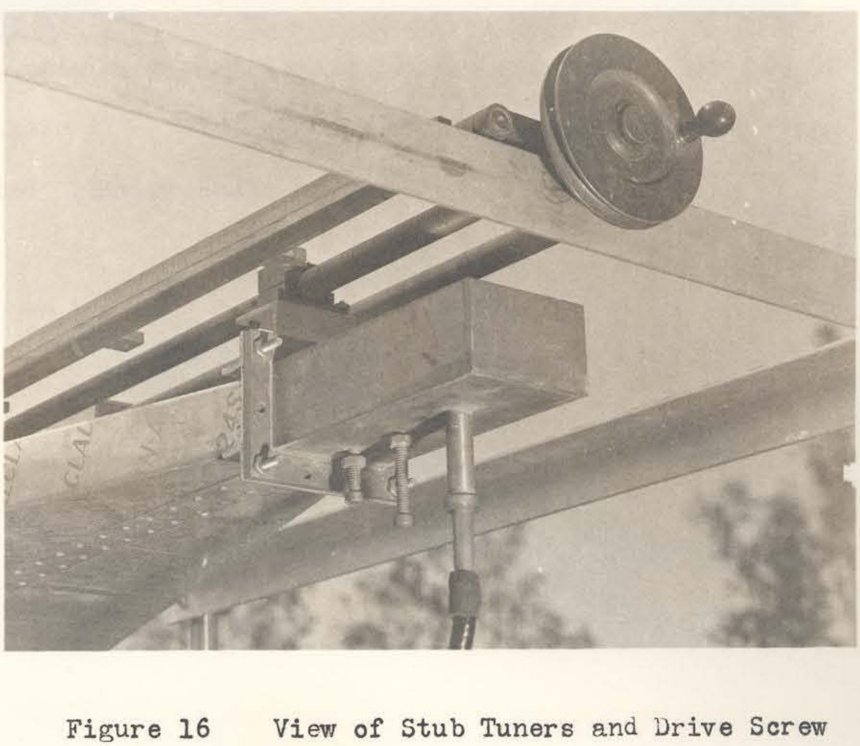

Figure 16 View of Stub Tuners and Drive Screw

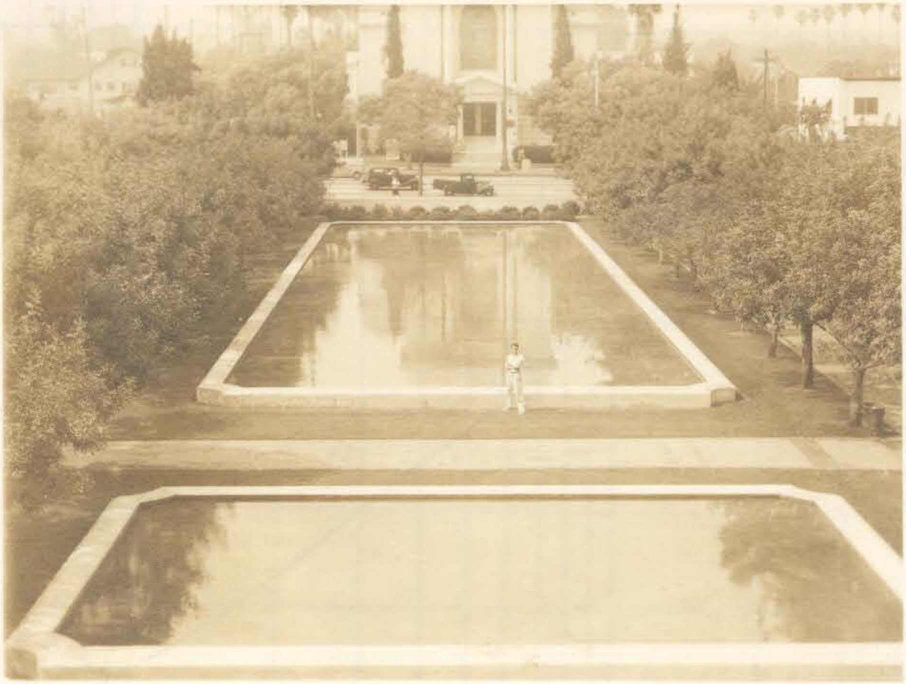

Figure 17 View of Pasadena City College Mirror Pond (background)

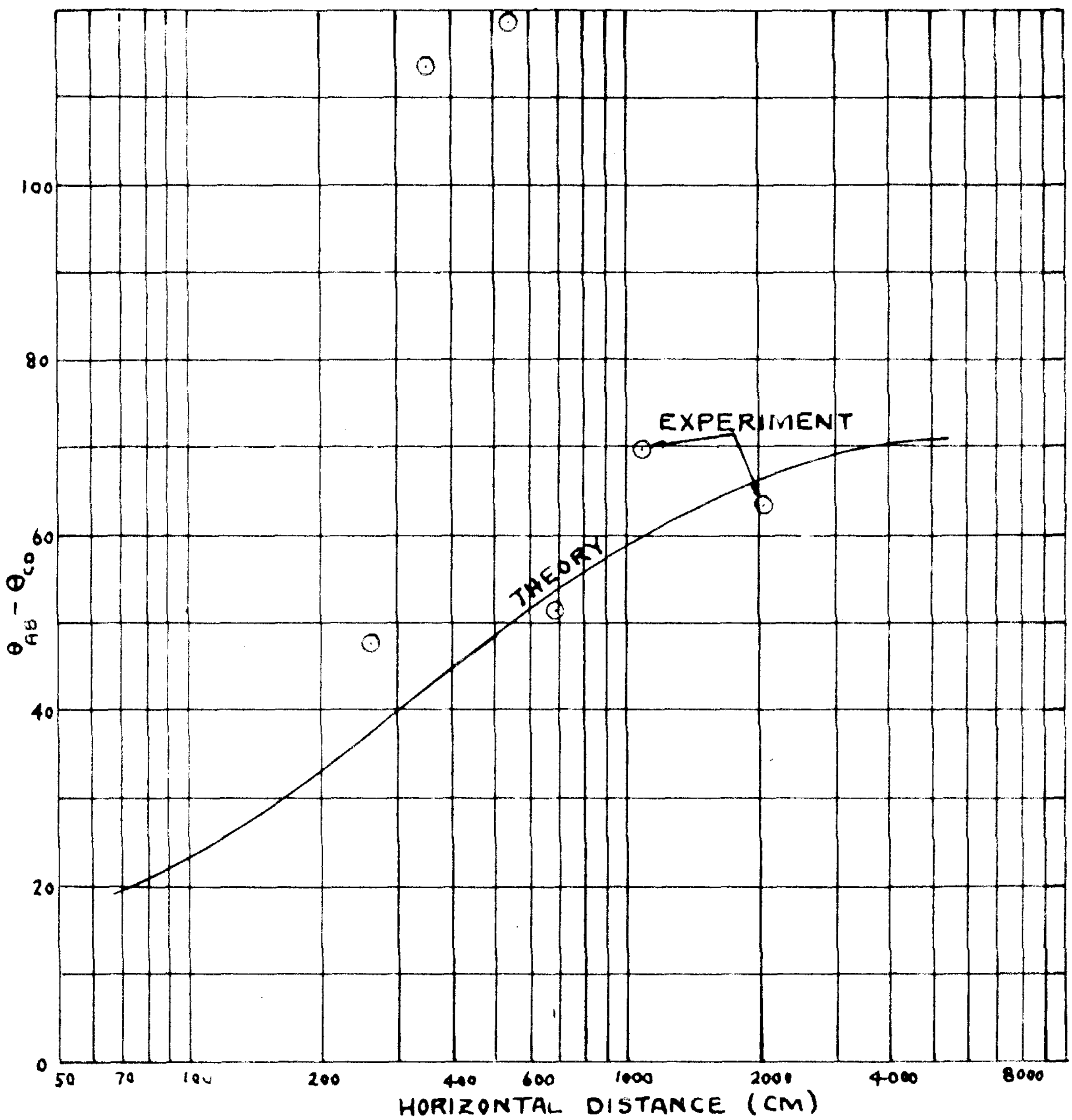

FIGURE 18 COMPARISON OF EXPERIMENTAL RESULTS WITH THEORY